Transport coefficients of Lennard-Jones fluids: A molecular-dynamics and effective-hard-sphere treatment

David M. Heyes
Department of Chemistry, Royal Holloway and Bedford New College, University of London, Egham, Surrey TW20 0EX, United Kingdom
(Received 29 July 1987)

This study evaluates the shear viscosity, self-diffusion coefficient, and thermal conductivity of the Lennard-Jones (LJ) fluid over essentially the entire fluid range by molecular-dynamics (MD) computer simulation. The Green-Kubo (GK) method is mainly used. In addition, for shear viscosity, homogeneous shear nonequilibrium MD (NEMD) is also employed and compared with experimental data on argon along isotherms. Reasonable agreement between GK, NEMD, and experiment is found. Hard-sphere MD modified Chapman-Enskog expressions for these transport coefficients are tested with use of a temperature-dependent effective hard-sphere diameter. Excellent agreement is found for shear viscosity. The thermal conductivity and, more so, self-diffusion coefficient is less successful in this respect. This behavior is attributed to the attractive part to the LJ potential and its soft repulsive core. Expressions for the constant-volume and -pressure activation energies for these transport coefficients are derived solely in terms of the thermodynamic properties of the LJ fluid. Also similar expressions for the activation volumes are given, which should have a wider range of applications than just for the LJ system.

I. INTRODUCTION

This work involves an evaluation of the shear viscosity, self-diffusion coefficient and thermal conductivity of the Lennard-Jones (LJ) fluid over a comprehensive range of its phase diagram. In the main equilibrium molecular dynamics (EMD) is used to obtain these transport coefficients (TC) using Green-Kubo (GK) formulas.[1,2] However, the method of homogeneous shear nonequilibrium molecular dynamics (NEMD) is also used for the shear viscosity,[3,4] on many of the state points to provide corroboration. Favorable comparisons with experimental values for the viscosity of argon are also made, using the Michels LJ parameters.[1]

Another objective of this work is to test a model for molecular fluid transport coefficients based on an assumed underlying hard-sphere fluid. This model is described in Sec. V. To predict all transport coefficients it requires essentially only one semiempirical parameter along each isotherm. Thus, for the LJ fluid we require a temperature-dependent effective hard-sphere diameter. We show that this has a sound physical basis for the shear viscosity but, at low temperatures there are departures from this model for the thermal conductivity and at high temperatures for the self-diffusion coefficient.

II. EQUATIONS OF MOTION AND IMPLEMENTATION

In this section the equations of motion used to determine the transport coefficients are described with emphasis on the algorithmic implementation.

A. EMD

The equations of motion for zero total momentum and constant kinetic energy N-molecule dynamics are[5-7]

$$\dot{\mathbf{q}}=\mathbf{p}/m \ , \tag{1}$$

$$\dot{\mathbf{p}}=m\ddot{\mathbf{q}}-\alpha\mathbf{P} \ , \tag{2}$$

$$K=\sum_{i=1}^{N}\mathbf{P}_i^2/2m \ , \tag{3}$$

$$\dot{K}=(K_0-K)/\tau \ , \tag{4}$$

and

$$K_0=(3N-4)k_BT/2 \ . \tag{5}$$

Here α is a Gaussian multiplier and m is the molecular mass, which are all the same here.

Using $\mathbf{q}_n$ as the generalized co-ordinate of a particle at time $t_n=nh$, where h is the magnitude of the time step. Then the Verlet "leap frog" algorithm for these equations of motion is

$$\mathbf{q}_{n+1}=\mathbf{q}_n+\mathbf{P}_{n+1/2}h/m \ , \tag{6}$$

$$\mathbf{P}_{n+1/2}=A\mathbf{P}_{n-1/2}+Bm\ddot{\mathbf{q}}_nh+O(h^3) \ , \tag{7}$$

$$\mathbf{P}_n=(\mathbf{P}_{n-1/2}+\tfrac{1}{2}m\ddot{\mathbf{q}}_nh)C+O(h^2) \ , \tag{8}$$

$$\ddot{\mathbf{q}}_{ni}=-\sum_{\substack{j=1\\ j\neq i}}^{N}(\mathbf{q}_{ij}/q_{ij})\frac{d\Phi}{dr} \ , \tag{9}$$

where

$$\mathbf{q}_{ij}=\mathbf{q}_i-\mathbf{q}_j \ , \tag{10}$$

$$A=1-\alpha h/(1+\alpha h/2) \ , \tag{11}$$

$$B=1-\alpha h/(2+\alpha h)\ , \tag{12}$$

$$C=1/(1+\alpha h/2)\ , \tag{13}$$

$$\alpha=D/(E+F)\ , \tag{14}$$

$$D=2(\nu/2\tau+\mu-\Theta/2\tau)\ , \tag{15}$$

$$E=\nu-h\mu/2+h\Theta/2\tau\ , \tag{16}$$

$$F=[\nu^2-h\nu(\mu-\Theta/\tau)+h^2(\mu^2/4+\Theta\nu/4\tau^2)]^{1/2}\ , \tag{17}$$

$$\mu=\sum_{i=1}^{N}\boldsymbol{\rho}_{ni}\cdot\ddot{\mathbf{q}}_{ni}\ , \tag{18}$$

$$\nu=\sum_{i=1}^{N}\boldsymbol{\rho}_{ni}^2/m\ , \tag{19}$$

$$\boldsymbol{\rho}_n=\boldsymbol{\rho}_{n-1/2}+\tfrac{1}{2}m\ddot{\mathbf{q}}_n h\ , \tag{20}$$

$$\boldsymbol{\rho}_{n+1/2}=\boldsymbol{\rho}_{n-1/2}+m\ddot{\mathbf{q}}_n h\ , \tag{21}$$

and

$$\Theta=(3N-4)k_B T\ . \tag{22}$$

A better estimate of the true velocity at t_n is given by[6]

$$\mathbf{V}_n=(a\mathbf{q}_{n+1}+b\mathbf{q}_n+c\mathbf{q}_{n-1}+d\mathbf{q}_{n-2})/h\ , \tag{23}$$

where a, b, c, and d are constants obtained from the Taylor expansion,

$$\mathbf{q}_{n+k}=\mathbf{q}_n+\mathbf{V}_n h_k+\tfrac{1}{2}\ddot{\mathbf{q}}_n h_k^2+\tfrac{1}{6}\dddot{\mathbf{q}}_n h_k^3+O(h_k^4)\ , \tag{24}$$

where

$$h_k=t_{n+k}-t_n\ , \tag{25}$$

and substituting Eqs. (24) and (25) in Eq. (23), giving $a=\frac{1}{3}$, $b=\frac{1}{2}$, $c-1$, and $d=\frac{1}{6}$. Hence,

$$\mathbf{V}_n=(2\mathbf{P}_{n+1/2}+5\mathbf{P}_{n-1/2}-\mathbf{P}_{n-3/2})/6m+O(h^3)\ . \tag{26}$$

(This step adds negligible time to the simulation because the $\mathbf{P}_{n-3/2}$ have already been evaluated.)

The system can be driven to a desired temperature T by substituting in Eqs. (15)–(17) a new definition for Θ in place of that given by Eq. (22), viz.,

$$\Theta=\Theta_0 T_u T/T_v^2\ , \tag{27}$$

where

$$\Theta_0=(3N-4)k_B T\ , \tag{28}$$

$$T_u=\left\langle\sum_{i=1}^{N}\mathbf{P}_{ni}^2/3m(N-\tfrac{4}{3})k_B\right\rangle\ , \tag{29}$$

using Eq. (8) and

$$T_v=\left\langle\sum_{i=1}^{N}\mathbf{V}_{ni}^2/3m(N-\tfrac{4}{3})k_B\right\rangle\ , \tag{30}$$

using Eq. (23) and $\langle\ldots\rangle$ denotes a local time average.

B. NEMD

A constant strain rate $\dot\gamma$ is applied to the system using SLLOD homogeneous shearing and Lees-Edwards periodic boundary conditions. Again, omitting the particle subscript i unless necessary,[5,7]

$$\dot\gamma=d\dot{\mathbf{q}}_x/dz\ . \tag{31}$$

The equations of motion (1) and (2) are replaced by

$$\dot{\mathbf{q}}=\mathbf{p}/m+\dot\gamma q_y\hat{\mathbf{x}}\ , \tag{32}$$

$$\dot{\mathbf{P}}=m\ddot{\mathbf{q}}-\dot\gamma P_y\hat{\mathbf{x}}-\alpha\mathbf{P}\ , \tag{33}$$

$$\alpha=[\mu-\gamma\kappa+(\nu-\Theta)/2\tau]/\nu\ , \tag{34}$$

$$\kappa=\sum_{i=1}^{N}\rho_{nxi}\rho_{nyi}/m\ , \tag{35}$$

$$\boldsymbol{\rho}_n=C[\mathbf{P}_{n-1/2}+(m\ddot{\mathbf{q}}_n-\dot\gamma P_{ny}\hat{\mathbf{x}})h/2]\ , \tag{36}$$

μ,ν and Θ are defined in (18), (19), and (27), respectively. Self-consistency between Eqs. (34)–(36) is obtained by iteration with α initially equated to zero. As

$$\boldsymbol{\rho}_{ny}=C(\mathbf{P}_{n-1/2,y}+m\ddot{\mathbf{q}}_{ny}h/2)\ , \tag{37}$$

then α cannot be written in the closed form of Eq. (14) when $\dot\gamma\neq 0$.

III. SIMULATION DETAILS

The EMD and NEMD simulations were performed with the algorithms supplied in Sec. II. The remaining features of the EMD and NEMD FORTRAN programs are given in recent articles.[1–4] First we consider EMD. The self-diffusion coefficient D is obtained from the mean-square displacements and equivalent Green-Kubo formula.[8]

$$D=\tfrac{1}{3}\lim_{t_c\to\infty}\int_0^{t_c}dt\,\langle\mathbf{V}_i(t)\mathbf{V}_i(0)\rangle f(t,t_c)\ , \tag{38}$$

where the V_i are defined by Eq. (26); strictly,

$$f(t,t_c)=1-t/t_c\ . \tag{39}$$

A route to D using essentially Eq. (38) that is economical on computer memory is described below.[9,10]

Define

$$\mathbf{I}_\alpha=\sum_{i=1}^{N}(-1)^i\mathbf{V}_{n\alpha i}\ , \tag{40}$$

then

$$D=\frac{N-1}{3N^2}\lim_{t_c\to\infty}\sum_{\alpha}\int_0^{t_c}dt\,\langle\mathbf{I}_\alpha(0)\mathbf{I}_\alpha(t)\rangle f(t,t_c)\ . \tag{41}$$

The factor of $(-1)^i$ in Eq. (39) ensures that the cross-velocity correlation function for finite N does not contribute to the $\mathbf{I}_\alpha$ auto correlation functions; only the velocity auto correlation function component contributes to $\langle I(0)I(t)\rangle$. The shear viscosity is derived from the off-diagonal component of the pressure tensor,[11]

$$\eta=\frac{V}{k_B T}\lim_{t_c\to\infty}\int_0^{t_c}dt\,\langle P_{\alpha\beta}(0)P_{\alpha\beta}(t)\rangle f(t,t_c)\ , \tag{42}$$

where V is the volume of the MD cell and

$$P_{\alpha\beta}=\frac{1}{V}\left[\sum_{i=1}^{N} mV_{\alpha i}V_{\beta i} - \frac{1}{2}\sum_{i=1}^{N}\sum_{\substack{j=1\\(j\neq i)}}^{N}\left[\frac{q_{\alpha ij}q_{\beta ij}}{q_{ij}}\right]\frac{d\Phi}{dr}\right] \quad \alpha\neq\beta , \tag{43}$$

$$q_{\alpha ij}=q_{\alpha i}-q_{\alpha j} , \tag{44}$$

and $q_{\alpha i}$ is the α-Cartesian component of $\mathbf{q}_i$. The "true" velocity components $V_{\alpha i}$ and $V_{\beta i}$ are taken from Eq. (26). The thermal conductivity λ is also obtained from a Green-Kubo (GK) relationship[12]

$$\lambda=\frac{V}{k_B T^2}\int_0^{t_c} dt\langle J_\alpha(0)J_\alpha(t)\rangle f(t,t_c) , \tag{45}$$

where

$$J_\alpha=\frac{1}{2V}\sum_{i=1}^{N}\left[V_{\alpha i}\left[m\mathbf{V}_i^2+\sum_{\substack{j=1\\(j\neq i)}}^{N}\Phi_{ij}\right]+V_{xi}\sum_{\substack{j=1\\(j\neq i)}}^{N}\frac{(q_{xij}q_{xij})}{q_{ij}}\Phi'_{ij}+V_{yi}\sum_{\substack{j=1\\(j\neq i)}}^{N}\frac{q_{xij}q_{yij}}{q_{ij}}\Phi'_{ij}+V_{zi}\sum_{\substack{j=1\\(j\neq i)}}^{N}\frac{(q_{xij}q_{zij})}{q_{ij}}\Phi'_{ij}\right] . \tag{46}$$

The GK integrals are integrated using Simpson's rule. This is essential for the large time steps chosen here.

A. Errors

The confidence limits of the mean of variables in a MD simulation can be evaluated taking into account the partial correlation between values at successive time steps.[13,14] Consider a property X, which could be pressure or stress for example, then the standard deviation of the time average of X, σ^{SD}, is defined by

$$\sigma^{\mathrm{SD}}=(\langle X^2\rangle-\langle X\rangle^2)^{1/2} , \tag{47}$$

and the standard error, $\sigma^{\mathrm{SE}'}$, by

$$\sigma^{\mathrm{SE}'}=\sigma^{\mathrm{SD}}\left[\frac{y}{(N_t-1)}\right]^{1/2} , \tag{48}$$

where N_t is the number of time steps and

$$y=\lim_{N_A\to\infty}(N_A\sigma_N^{\mathrm{SD}^2}/\sigma^{\mathrm{SD}^2}) , \tag{49}$$

where

$$\sigma_N^{\mathrm{SD}}=\langle\langle X_N^2\rangle-\langle X_N\rangle^2\rangle^{1/2} . \tag{50}$$

X_N is the average of property X over N_A consecutive time steps (N_A is 200 time steps here). The sequence of N_A time steps are contiguous. Therefore, the "true" standard error, $\sigma^{\mathrm{SE}'}$, for the shear viscosity in continuous shear NEMD is given by

$$\sigma^{\mathrm{SE}'}(\eta)=\sigma^{\mathrm{SE}'}(P_{xy})/\dot{\gamma} . \tag{51}$$

Another estimate for $\sigma^{\mathrm{SE}'}(\eta)$ by NEMD was derived by Gillan;[15]

$$\sigma^{\mathrm{SE}'}(\eta)=(2\rho k_B T\langle\eta\rangle/Nt_{\mathrm{sim}})^{1/2}\dot{\gamma}^{-1} , \tag{52}$$

where t_{sim} is the duration of the simulation. For example, using $\rho=1.0$, $T=2.0$, $\eta=3$, $\dot{\gamma}=0.1$, $N=256$, and $\Delta t=0.02$ one requires 5200 time steps to obtain 5% confidence in the shear viscosity. The collective property transport coefficients, Z, ($=\eta$ or λ) are also evaluated here by EMD using the Green-Kubo integrals. In this case the error estimates are less well defined. If the reasonable assumption is made that the significant dynamical processes are Gaussian at times comparable to those required to assign the transport coefficients,[16] then[17]

$$\sigma^{\mathrm{SE}'}[Z(t)]\lesssim nt\langle Z\rangle/(t_{\mathrm{sim}}\tau)^{1/2} , \tag{53}$$

where $n=4$ or 2 as given below and where

$$Z(t)=A\int_0^t dt^1\langle Z(0)Z(t^1)\rangle , \tag{54}$$

A is a constant and τ is a correlation time ($\approx\eta/G_\infty$). For self-diffusion,

$$\sigma^{\mathrm{SE}'}[D(t)]<4t\langle D\rangle/(Nt_{\mathrm{sim}}\tau)^{1/2} , \tag{55}$$

and

$$D(t)=\int_0^t dt^1\langle V_\alpha(0)V_\alpha(t^1)\rangle . \tag{56}$$

Similarly for shear viscosity,[17]

$$\sigma^{\mathrm{SE}'}[\eta(t)]\lesssim 2t\langle\eta\rangle/(t_{\mathrm{sim}}\tau)^{1/2} . \tag{57}$$

Note that the standard error for $\eta(t)$ is independent of N. The only advantage in increasing the size of the MD cell is to eliminate N dependencies introduced by the periodic boundary conditions. To obtain 5% accuracy in η using $t=0.5$, $\tau=0.2$, and $\Delta t=0.02$ LJ reduced units then 100 000 time steps are required.

IV. SIMULATION RESULTS

Using the methods described in Secs. II and III, computations were performed on cubic MD cells containing 108, 256, 500 molecules and for the NEMD simulations 256 and 2048 Lennard-Jones (12-6) molecules at LJ reduced densities greater than 0.2 and temperatures $0.7\lesssim kT/\varepsilon\lesssim 10$. The production simulations, during which the viscosity and related properties were accumulated, were conducted for Ca; 4×10^5, 1.5×10^5, and 1.5×10^5 time steps for $N=108$, 256, and 500 at equilibrium. The NEMD simulations ran for approximately 8×10^4 and 2×10^4 for $N=256$ and 2048. The time steps were 0.022 $\rho/T^{1/2}$; a prescription incorporated within the MD program. Derived quantities reported in this work are measured in LJ reduced units of ε for energy, m for mass, and σ_{LJ} for distance. Hence for temperature ε/k_B (k_B is the Boltzmann constant), $\sigma_{\mathrm{LJ}}(m/\varepsilon)^{1/2}$ for time, $(m/\varepsilon)^{-1/2}/\sigma_{\mathrm{LJ}}$ for the shear rate, $\varepsilon/\sigma_{\mathrm{LJ}}^3$ for the pressure

TABLE I. Thermodynamic, mechanical, and dynamical aspects of MD simulated LJ states.

ρ[a]	T[b]	N[c]	U[d]	P[e]	G_∞[f]	η_e[g]	η_G[h]	η_N[i]	D[j]	λ[k]	λ_N[l]
0.835	0.72	108	−4.99	−0.17	22.6		2.8		0.031	6.4	
0.835	0.72	256	−4.98	−0.10	22.8		3.05		0.031	6.7	
0.848	0.72	108	−5.08	−0.00	23.8		3.2		0.026	6.7	
0.848	0.72	256	−5.05	0.14	24.1		3.5		0.029	6.9	
0.848	0.72	500	−5.05	0.12	24.1		3.4		0.029	6.5	
0.864	0.72	256	−5.16	0.35	25.7		3.8		0.023	6.8	
0.884	0.72	108	−5.31	0.59	27.6		4.6		0.018	7.2	
0.884	0.72	256	−5.28	0.74	27.9		4.8		0.019	7.4	
0.916	0.72	108	−5.51	0.26	28.4		> 18.0		0.012	7.4	
0.916	0.72	256	−5.60	0.65	30.0		7.5		0.013	8.2	
0.801	0.81	108	−4.54	−0.05	20.6		2.2		0.045	5.8	
0.864	0.81	108	−4.94	0.85	26.6		3.3		0.028	6.9	
0.864	0.81	256	−4.92	0.96	26.9		3.65		0.029	7.0	
0.864	0.81	500	−4.91	0.99	27.0		3.6		0.031	7.6	
0.884	0.81	108	−5.06	1.25	28.9		3.9		0.023	7.5	
0.884	0.81	500	−5.07	1.12	28.6		3.9		0.022	7.7	
0.916	0.81	108	−5.57	0.44	29.6		> 30.0		0.002	7.1	
0.916	0.81	256	−5.46	0.75	30.1		2.3		0.003	7.7	
0.916	0.90	256	−4.94	2.90	34.7		5.1		0.021	8.0	
0.916	0.95	108	−4.84	3.07	35.0		4.9		0.023	8.4	
0.400	1.06	256	−1.37	−0.01	4.5		0.37		0.31	1.9	
0.679	1.06	108	−3.14	0.04	14.1		1.1		0.11	4.1	
0.679	1.06	256	−3.13	0.06	14.1		1.1		0.12	3.9	
0.679	1.06	500	−3.13	0.06	14.1		1.1		0.12	4.2	
0.700	1.06	256	−3.27	0.17	15.4		1.2		0.12	4.4	
0.731	1.06	108	−3.49	0.38	17.4		1.36		0.089	4.75	
0.731	1.06	256	−3.48	0.40	17.4		1.3		0.091	4.95	
0.769	1.06	108	−3.74	0.76	20.3		1.7		0.073	5.6	
0.769	1.06	256	−3.73	0.79	20.4		1.7		0.079	5.5	
0.821	1.06	108	−4.06	1.53	25.0		2.2		0.055	6.8	
0.821	1.06	256	−4.04	1.58	25.2		2.3		0.059	6.4	
0.821	1.06	500	−4.03	1.60	25.2		2.4		0.060	6.7	
0.848	1.06	500	−4.18	2.16	28.1		2.67		0.052	7.0	
0.88	1.06	500	−4.34	2.97	32.0		3.3		0.042	8.0	
0.91	1.06	500	−4.47	3.87	36.1		4.1		0.035	9.2	
0.916	1.1	108	−4.43	4.14	37.1		4.1		0.030	8.8	
0.916	1.1	256	−4.39	4.31	37.5		4.2		0.033	8.9	
0.916	1.2	256	−4.13	4.98	38.8		4.4		0.040	8.9	
0.4000	1.35	108	−0.72	0.14	4.58		0.39		0.38	1.8	1.8
0.4000	1.35	256	−0.69	0.16	4.64		0.37		0.40	1.8	
0.6000	1.35	108	−1.98	0.46	11.3		0.80		0.20	3.5	3.5
0.6000	1.35	256	−2.01	0.44	11.3		0.79		0.20	3.4	
0.6000	1.35	500	−2.01	0.44	11.3		0.84		0.21	3.4	
0.7000	1.35	256	−2.66	1.09	17.1		1.2		0.14	4.6	
0.8000	1.35	256	−3.23	2.57	25.7		1.9		0.090	6.4	6.3
0.8000	1.35	500	−3.23	2.57	25.7		2.0		0.094	6.3	
0.8600	1.35	500	−3.52	4.04	32.7		2.7		0.063	7.7	
0.9000	1.35	108	−3.71	5.22	38.0		3.2		0.048	8.4	
0.916	1.4	108	−3.64	6.12	41.0		3.6		0.047	9.1	
0.916	1.4	256	−3.60	6.26	41.3		3.7		0.050	8.9	
0.3000	1.4562	256	0.17	0.22	2.71		0.30		0.69	1.45	
0.4000	1.4562	256	−0.52	0.23	4.72		0.48		0.45	1.8	
0.5249	1.4562	256	−1.32	0.39	8.46	0.65	0.64	0.65	0.28	2.6	
0.5708	1.4562	256	−1.62	0.53	10.3	0.76	0.78	0.75	0.23	3.0	
0.6178	1.4562	256	−1.92	0.75	12.6	0.90	0.89	0.87	0.21	3.6	
0.7636	1.4562	256	−2.81	2.30	23.0	1.6	1.6	1.6	0.11	5.95	
0.8630	1.4562	108	−3.31	4.59	33.9	2.7	2.5		0.066	7.6	

TABLE I. (*Continued*).

ρ[a]	T[b]	N[c]	U[d]	P[e]	G_∞[f]	η_e[g]	η_G[h]	η_N[i]	D[j]	λ[k]	λ_N[l]
0.8630	1.4562	256	−3.28	4.66	34.1	2.7	2.7	2.8	0.071	7.9	
0.8630	1.4562	500	−3.27	4.69	34.2	2.7	2.7		0.069	8.3	
0.8969	1.4562	108	−3.44	5.72	38.7	3.3	3.0		0.054	8.5	
0.8969	1.4562	256	−3.39	5.92	39.1	3.3	3.3	3.3	0.062	8.9	
0.8969	1.4562	500	−3.39	5.87	39.0	3.3	3.3		0.059	9.0	
0.9112	1.4562	108	−3.48	6.27	40.9	3.7	3.3		0.051	9.0	
0.9112	1.4562	256	−3.43	6.48	41.3	3.7	3.6	3.6	0.058	9.6	
0.9380	1.4562	108	−3.56	7.40	45.3	4.4	4.0		0.043	9.8	
0.9380	1.4562	256	−3.49	7.67	45.8	4.4	4.0	4.3	0.047	10.3	
0.9380	1.4562	500	−3.50	7.62	45.7	4.4	4.25		0.050	10.5	
0.9618	1.4562	256	−3.53	8.89	50.2	5.0	4.7	5.3	0.038	10.7	
0.9832	1.4562	256	−3.57	10.0	54.3		5.6		0.033	11.3	
0.9933	1.4562	256	−3.58	10.6	56.3	6.3	6.5	6.3	0.031	11.2	
1.0017	1.4562	256	−3.58	11.1	58.1	6.75	7.3	6.8	0.028	11.3	
0.916	1.5000	256	−3.35	6.86	42.4		3.5		0.053	9.1	
0.916	1.7000	108	−2.88	7.93	44.5		3.3		0.061	9.4	
0.916	1.7000	256	−2.84	8.04	44.7		3.7		0.061	10.0	
0.2000	1.8627	256	1.44	0.28	1.38		0.3		1.3	1.3	
0.3000	1.8627	256	0.83	0.41	2.91		0.35		0.78	1.5	
0.4000	1.8627	256	0.21	0.58	5.18		0.47		0.53	2.1	
0.5000	1.8627	256	−0.41	0.88	8.44		0.61		0.37	2.6	
0.6000	1.8627	256	−1.03	1.46	13.1		0.88	0.83	0.26	3.4	
0.7000	1.8627	256	−1.60	2.60	19.9		1.2	1.2	0.184	5.0	
0.8010	1.8627	108	−2.11	4.66	29.8	2.1	1.9		0.12	6.7	
0.8010	1.8627	256	−2.09	4.70	29.9	2.1	2.0	1.9	0.12	7.0	
0.8010	1.8627	500	−2.08	4.73	29.9	2.1	2.0		0.13	7.4	
0.8724	1.8627	256	−2.34	7.05	39.4	2.9	2.7	2.7	0.095	8.9	
0.9248	1.8627	108	−2.49	9.27	47.8	3.6	3.2		0.06	9.9	
0.9248	1.8627	256	−2.45	9.40	48.0	3.6	3.44	3.5	0.071	10.2	
0.9248	1.8627	500	−2.43	9.47	48.1	3.6	3.45		0.072	10.0	
0.9659	1.8627	108	−2.54	11.5	55.6	4.7	4.2		0.052	11.2	
0.9659	1.8627	256	−2.46	11.8	56.2	4.7	4.3	4.4	0.056	11.8	
1.0004	1.8627	256	−2.44	14.2	63.9	5.8	5.35	5.7	0.049	12.1	
1.0153	1.8627	108	−2.53	14.8	66.5	6.3	5.9		0.038	11.7	
1.0153	1.8627	256	−2.42	15.3	67.4	6.3	6.2	6.2	0.043	13.1	
1.0153	1.8627	500	−2.42	15.2	67.3	6.3	6.4		0.043	12.7	
1.0236	1.8627	256	−2.40	16.0	69.5	7.0	7	6.4	0.044	12.8	
1.0290	1.8627	256	−2.39	16.4	70.9	7.3	6.7	6.9	0.040	12.9	
1.0367	1.8627	256	−2.39	16.9	72.6	7.9	7.4	6.9	0.03	14.0	
1.0391	1.8627	256	−2.38	17.1	73.3	7.95	7.4	7.3	0.035	13.9	
1.0415	1.8627	256	−2.39	17.3	73.8	8.5	7.5	8.2	0.037	13.9	
1.0438	1.8627	256	−2.38	17.6	74.7	8.5	8.2	8.2	0.034	13.4	
1.0468	1.8627	256	−2.38	17.7	75.2	8.4	8.0	7.9	0.033	13.4	
0.3000	1.95	256	0.99	0.46	2.98		0.35		0.81	1.6	1.7
0.5000	1.96	108	−0.26	0.99	8.6		0.62		0.36	2.6	2.9
0.5000	1.99	256	−0.18	1.04	8.72		0.62		0.40	2.6	
0.6000	2.0000	108	−0.79	1.72	13.6		0.85		0.29	3.6	3.8
0.6000	2.0000	256	−0.75	1.75	13.7		0.85		0.30	3.7	
0.8000	2.0000	500	−1.77	5.24	30.8		1.8		0.15	7.2	7.3
1.0400	2.0000	108	−2.12	17.17	74.5		6.3		0.036	12.8	13.2
0.916	2.1	256	−1.84	10.35	49.1		3.2		0.087	10.4	
0.916	2.3	256	−1.36	11.39	51.0		3.3		0.099	10.4	
0.3000	2.45	256	1.83	0.71	3.31		0.42	0.36	0.97	1.6	
0.4000	2.5138	256	1.34	1.12	5.99		0.49	0.48	0.77	2.3	
0.5000	2.5138	256	0.77	1.72	9.83		0.67	0.65	0.46	3.0	
0.6594	2.29	108	−0.56	3.06	18.7	1.15	1.1		0.25	4.75	
0.7195	2.5138	256	−0.37	4.80	25.1	1.4	1.3	1.4	0.23	6.1	

TABLE I. (*Continued*).

ρ[a]	T[b]	N[c]	U[d]	P[e]	G_∞[f]	η_e[g]	η_G[h]	η_N[i]	D[j]	λ[k]	λ_N[l]
0.7653	2.5138	256	−0.55	6.00	30.0	1.6	1.6	1.6	0.19	6.45	
0.8028	2.5138	256	−0.67	7.21	34.7	1.9	1.8	1.9	0.18	7.2	
0.8028	2.4964	500	−0.70	7.18	34.6	1.9	2.0		0.17	7.6	
0.8344	2.4884	108	−0.84	8.29	38.9	2.1	2.1		0.15	8.2	
0.8344	2.5138	108	−0.79	8.36	39.0	2.1	2.1		0.15	7.7	
0.8344	2.5138	256	−0.75	8.43	39.2	2.1	2.1	2.1	0.15	8.4	
0.8344	2.5138	500	−0.74	8.43	39.1	2.1	2.1		0.16	8.4	
0.8623	2.5138	108	−0.84	9.54	43.3	2.45	2.3		0.14	8.7	
0.8623	2.5138	256	−0.81	9.61	43.4	2.45	2.3	2.4	0.14	8.4	
0.8623	2.5138	500	−0.80	9.64	43.5	2.45	2.4		0.14	9.2	
0.8873	2.5138	256	−0.83	10.9	47.8	2.7	2.6	2.7	0.12	9.5	
0.9093	2.5138	256	−0.84	12.1	51.8	2.9	2.95	3.0	0.12	10.4	
0.9093	2.5138	500	−0.84	12.1	51.7	2.9	3.0		0.12	10.4	
0.9200	2.5138	108	−0.91	12.5	53.5	3.1	3.0		0.10	10.0	
0.9200	2.5138	256	−0.85	12.7	53.9	3.1	3.2	3.0	0.11	11.0	
0.9200	2.5138	500	−0.84	12.7	53.8	3.1	3.2		0.11	11.1	
0.9200	2.5138	500	−0.84	12.7	53.8	3.1	3.2		0.11	10.8	
0.9302	2.5138	256	−0.84	13.4	55.9	3.2	3.2	3.2	0.10	10.8	
0.9302	2.5008	500	−0.87	13.3	55.7	3.2	3.1		0.10	10.4	
0.9486	2.5138	256	−0.83	14.5	59.8	3.5	3.5	3.6	0.097	11.0	
0.9665	2.5138	108	−0.89	15.5	63.2	3.8	3.7		0.084	11.1	
0.9665	2.5138	256	−0.81	15.8	63.7	3.8	3.8	3.9	0.089	11.9	
0.9665	2.5138	500	−0.81	15.8	63.7	3.8	3.95		0.089	11.9	
0.9831	2.5138	256	−0.79	17.0	67.5	4.1	4.4	4.1	0.078	12.6	
0.9986	2.5138	108	−0.83	18.0	70.8	4.4			0.071	12.2	
0.9986	2.5138	256	−0.77	18.2	71.2	4.4	4.4	4.6	0.073	12.8	
0.9986	2.5138	500	−0.74	18.25	71.4	4.4	4.6		0.078	12.6	
1.0135	2.5138	108	−0.80	19.2	74.6	4.7	4.6		0.065	12.9	
1.0135	2.5138	256	−0.73	19.4	75.0	4.7	5.0	4.7	0.066	13.1	
1.0135	2.5138	500	−0.73	19.5	75.1	4.7	5.0		0.067	13.2	
1.0397	2.5138	108	−0.72	21.5	81.7	5.3	5.2		0.056	14.1	
1.0397	2.5138	256	−0.63	21.8	82.2	5.3	5.95	6.0	0.059	13.8	
0.3000	2.6974	256	2.18	0.82	3.47		0.44		0.98	2.0	
0.4000	2.6974	256	1.65	1.27	6.22		0.53		0.71	2.4	
0.5000	2.6974	256	1.08	1.94	10.2		0.66		0.50	3.2	
0.5463	2.6974	256	0.83	2.38	12.6	0.78	0.79	0.79	0.47	3.7	
0.6374	2.6974	256	0.36	3.61	18.6	1.07	1.06	1.02	0.33	4.6	
0.6993	2.6974	256	0.08	4.83	24.0	1.3	1.2	1.3	0.26	5.4	
0.7469	2.6974	256	−0.10	6.05	29.0	1.5	1.5	1.5	0.22	6.1	
0.7469	2.6974	500	−0.09	6.06	29.0	1.5	1.5		0.215	6.3	
0.7856	2.6974	256	−0.23	7.27	33.6	1.8	1.7	1.8	0.20	6.8	
0.8183	2.6974	256	−0.31	8.48	38.1	2.1	2.0	2.0	0.18	7.6	
0.8468	2.6974	256	−0.37	9.67	42.3	2.3	2.2	2.3	0.15	8.8	
0.8724	2.6974	256	−0.41	10.9	46.5	2.6	2.2	2.6	0.13	8.9	
0.8951	2.6974	256	−0.42	12.1	50.6	2.8	2.7	2.7	0.127	9.6	
0.8951	2.6974	500	−0.41	12.1	50.7	2.8	2.8		0.133	9.2	
0.9159	2.6974	256	−0.43	13.3	54.6	3.1	3.0	3.0	0.11	10.5	
0.9355	2.6974	256	−0.40	14.6	58.8	3.3	3.4	3.2	0.11	10.8	
0.9534	2.6974	256	−0.38	15.9	62.7	3.6	3.5	3.6	0.106	12.2	
0.9700	2.6974	256	−0.35	17.1	66.5		3.5	4.1	0.098	11.9	
0.9900	2.6974	256	−0.30	18.7	71.4		4.1	4.2	0.086	12.6	
1.0100	2.6974	108	−0.32	20.1	76.0		4.6		0.074	12.8	
1.0100	2.6974	256	−0.26	20.3	76.4		4.5	4.7	0.079	13.0	
1.0100	2.6974	500	−0.24	20.4	76.5		4.5		0.077	13.4	
1.0300	2.6974	256	−0.18	22.2	81.9		5.0	5.3	0.071	13.6	
1.0300	2.6974	500	−0.17	22.2	81.9		5.2		0.073	14.0	
1.0600	2.6974	108	−0.22	25.8	91.9		5.6	6.4	0.058	14.6	
1.1300	2.74	108	0.43	33.6	114		9.5		0.038	16.4	
1.1300	2.74	256	−0.87	26.2	99.5	FCC			0.00	16.1	

TABLE I. (*Continued*).

ρ[a]	T[b]	N[c]	U[d]	P[e]	G_∞[f]	η_e[g]	η_G[h]	η_N[i]	D[j]	λ[k]	λ_N[l]
0.916	3.0	256	0.28	14.8	57.3		3.1		0.13	11.0	
0.5463	5.85	256	6.31	8.38	22.7		1.2		0.62	5.6	
0.6374	5.85	256	6.23	9.51	28.8		1.22		0.60	6.4	
0.3000	6.0	256	7.58	2.45	5.76		0.59		1.6	2.0	
0.4000	6.0	256	7.17	3.82	10.1		0.71		1.15	3.6	
0.5000	6.0	256	6.82	5.74	16.4		0.88		0.87	4.4	
0.5463	6.0	256	6.69	6.88	20.1		1.1	1.1	0.74	5.8	
0.6374	6.0	256	6.50	9.76	29.2		1.34	1.2	0.63	6.1	
0.8183	6.0	256						2.1	0.35		
0.8468	6.0	256	6.63	21.3	63.1		2.34	2.2	0.37	10.3	
0.8468	5.9	500	6.48	21.0	62.7		2.2		0.36	9.2	
0.8724	6.0	256	6.73	23.4	69.0		2.3		0.30	10.9	
0.8951	6.0	256	6.83	25.3	74.4		2.54	2.7	0.29	11.0	
0.9159	6.0	256	6.93	27.3	79.8		2.8	2.8	0.29	11.6	
0.9355	6.0	256	7.04	29.2	85.1		2.9	2.9	0.25	11.5	
0.9534	6.0	256	7.18	31.2	90.5		3.0	3.2	0.24	13.9	
0.9700	6.0	256	7.30	33.1	95.5		3.5	3.4	0.26	12.9	
0.9700	6.0	500	7.32	33.1	95.5		3.5	3.3	0.25	12.9	
0.9900	6.0	256	7.47	35.6	102.0		3.4	3.5	0.22	13.9	
1.0100	5.88	108	7.25	37.2	107.1		3.7		0.20	14.4	
1.0100	6.0	256	7.65	38.1	108.7		3.8	3.9	0.22	15.0	
1.0100	6.0	500	7.66	38.1	108.6		3.9		0.22	15.2	
1.0300	6.0	256	7.85	40.9	115.9		4.0	4.2	0.21	15.4	
1.0300	5.96	500	7.75	40.6	115.3		4.1		0.22	16.0	
1.0600	6.0	108	8.01	44.8	126.4		4.2		0.16	15.2	
1.0600	6.0	256	8.17	45.3	127.2		4.3	4.8	0.19	16.2	
1.0600	6.0	500	8.18	45.3	127.1		5.0		0.185	52.8	
1.1800	6.0	256	9.99	67.8	183.4		7.2	7.2	0.12	21.9	
0.4000	10.0	256	13.8	6.68	14.3		0.98		1.7	4.3	
0.5000	9.98	256	13.6	9.87	22.8		1.1	1.1	1.3	4.6	
0.6000	10.0	256	13.7	14.3	34.5		1.3	1.3	1.0	6.4	
0.7000	10.0	256	13.9	20.2	50.2		1.7	1.7	0.79	7.7	
0.8000	10.0	256	14.3	28.3	71.2		2.0	2.1	0.63	9.7	
0.9000	10.0	256	15.1	39.2	98.8		2.6	2.8	0.49	12.4	
1.0000	9.68	256	15.6	52.6	132.8		3.6	3.6	0.35	14.9	
1.0400	10.0	256	16.9	60.8	151.9		4.7	4.1	0.34	16.8	
1.0800	10.0	256	17.6	68.8	171.0		4.5	4.5	0.30	18.0	
1.1200	10.0	256	18.4	77.6	192.1		5.3	5.3	0.27	20.0	
1.1800	10.0	256	19.8	93.1	228.2		6.2	6.5	0.23	23.0	
1.2200	10.0	256	20.9	104.7	255.0		6.9	7.6	0.19	25.0	

[a] ρ, reduced LJ density is equal to $N\sigma^3/V$.
[b] T, reduced LJ temperature is equal to k_BT/ε.
[c] N, number of molecules in the cell of volume V.
[d] U, configurational energy per molecule.
[e] P, pressure.
[f] G_∞, infinite frequency shear rigidity modulus.
[g] η_e, experimental value from argon, (Refs. 22 and 31) where $\varepsilon/k_B=119.8$ K and $\sigma=0.3405$ nm.
[h] η_G, the shear viscosity from the Green-Kubo expression, Eq. (42).
[i] η_N, the shear viscosity by NEMD, SLLOD homogeneous shear and extrapolation to zero shear rate (Ref. 3).
[j] D, the self-diffusion coefficient from Eq. (38) and the mean-square displacement (Ref. 1).
[k] λ, the thermal conductivity from Green-Kubo, Eq. (45).
[l] λ_N from a homogeneous NEMD method (Ref. 41).

and moduli tensorial components, and $(m\varepsilon)^{1/2}/\sigma_{\rm LJ}^2$ for the viscosity. The methods for estimating the standard errors of η given in Eqs. (48) and (52) agree well for the viscosities. In obtaining the Newtonian viscosity from a single run it is necessary to choose a shear rate that is small enough to eliminate shear thinning and yet large enough to produce a statistically significant nonzero shear stress and hence shear viscosity from $\eta=-P_{\alpha\beta}/\dot\gamma$. The optimum choice discovered was in the range from approximately $\dot\gamma=0.3T^{1/2}$ at $\rho=0.2$ to $\gamma=0.05T^{1/2}$ at $\rho=1.0$.

Table I contains the system properties for the LJ state

points considered in this work. The internal energy U, presure P, and shear rigidity modulus G_∞ are given. These are derived from the pair potential components to the internal energy and from formula,[1]

$$G_\infty = (V/k_B T)\langle P^2_{\alpha\beta}(0)\rangle \ .$$

Three routes to the Newtonian viscosity are given. Using the Michels LJ parameters: $\varepsilon/k_B = 119.8$ K and $\sigma_{LJ} = 0.3405$ nm, then experimental viscosities on argon can be converted into a "nearest-equivalent" Lennard-Jones fluid. In addition, the Green-Kubo expression gives $\eta(\dot\gamma \to 0)$ explicitly. The NEMD route requires an extrapolation of $\eta(\dot\gamma)$ to zero shear rate, which was performed graphically as seen in the examples of Fig. 1. Note that a significant degree of shear thinning, evident from the spanned density, temperature and shear rate range is confined to a comparatively narrow portion of the phase diagram at high density and low temperature. No noticeable N dependence was observed for the NEMD calculations. For viscosities $\gtrsim 3$ but less than ~ 5 the Green-Kubo method did show a small N dependence but of a largely random nature as Fig. 2 reveals. The viscosity increases by several percent on increasing N from 108 to 500, however, for viscosities $\gtrsim 5$. The self-diffusion coefficients and thermal conductivities increase by roughly the same proportion. This is due to a diminished limitation on the long wave length density fluctuations with increasing N. It is interesting to note from Fig. 2 that although the normalized time correlation functions show little evidence of an N dependence, the derived GK integrals do show some ("random") N dependence. Therefore the difference between the various N values lies in the mean square values for the velocity, shear stress and heat current, and not in their subsequent time evolution. As is revealed in Table I the three methods for obtaining the viscosity in the limit of zero shear rate agree very well. Only for viscosities greater than ~ 4 do statistical uncertainties and a (small) underestimation by GK cause noticeable differences between the three values. Even with these limitations the data is believed to be sufficiently accurate to test the model proposed in Sec. V.

The self-diffusion coefficients were obtained from Eq. (41) using $f(t,t_c)=1$ (same for all the GK expressions). The values obtained from the equivalent mean square displacement, msd, expression were in agreement with these. The msd formula[1] was employed by taking a single time origin for each molecule, persisting for the whole simulation. The msd route was not as statistically efficient as the GK route, which took time origins every time step. In Figs. 3 and 4 we show representative time correlation functions and their integrals, which demonstrate their state point dependence. As the temperature increases these functions become more short ranged and there is little problem in assigning a plateau value in the GK integral. As temperature increases, Fig. 5 reveals that the normalized shear stress autocorrelation function becomes largely density independent, in comparison with the velocity and heat current autocorrelation functions. The shear viscosity would appear to be the most readily included within a simple mechanistic framework.

If the Newtonian viscosity is required and in LJ reduced units it is $\lesssim 3T^{1/2}$, that is, it is not too close to the fluid-solid phase change then the GK method is preferred to NEMD because it only requires a single simulation (to ensure linear behavior) and also all transport coefficients can be obtained simultaneously. The NEMD method is favored in the gas phase because the approach to linearity is weakly shear rate dependent ($\sim\dot\gamma^2$) and the GK approach is hampered by long relaxation times in the time correlation functions. Both methods have problems close to the (important) regime close to the fluid-solid transition. GK has an increasing N dependence and develops a long-time tail in the ACF. The NEMD method, although it does not appear to have an N dependence, has a disputed analytic form for the shear rate dependence of η. If one uses the observation that linearity can be assumed for $\dot\gamma \lesssim 0.1\, G_\infty/\eta$ then the ratio of standard errors for NEMD to EMD is $\alpha\eta\rho^{1/2}T^{1/2}$ from Eqs. (52) and (57). It suggests that the EMD route would be favored in this region. However, the error estimates based on Eqs. (52) and (57) do not incorporate N dependencies in EMD arising from the periodic boundary conditions. The relative merits of EMD and NEMD in this part of the phase diagram have still therefore to be clarified.

Below we investigate the possibility of reconciling these three transport coefficients within a common soundly based theoretical framework.

V. EFFECTIVE HARD-SPHERE MODEL

There have been many semiempirical expressions relating the TC to the thermodynamic state variables; usually the free volume.[18,19] In this spirit we also relate the LJ transport coefficients to the available free volume of an underlying natural reference fluid—the hard-sphere fluid. The transport properties of the hard-sphere fluid are known almost exactly in terms of the free volume in the region of the phase diagram of interest here, using MD corrected Chapman-Enskog (CE) formulas.[20–22] These expressions can be applied to the LJ fluid by adopting a temperature dependent effective hard-sphere diameter for each LJ molecule. The reduced density of the LJ system in terms of the hard-sphere diameter can then be employed in the equations for the hard-sphere transport coefficients. The Dymond procedure for choosing the effective hard-sphere diameter from the shear viscosities is used.[23] The CE formulas express the transport coefficients as a product of a temperature and a density dependent term. The same formulas can be applied to the LJ fluid. (Although the density dependent term involves a density scaled by the temperature-dependent hard-sphere diameter, so it is not entirely temperature independent.) This parametrization is readily extended to give sample expressions for the constant volume and pressure activation energies for shear viscosity, together with the pressure viscosity coefficient and derived activation volume in terms of the thermodynamics of the original LJ fluid. (Similar expressions can be derived for D and λ.) Implicit in this solution is that one can isolate the effects of temperature and pressure on the transport coefficients of the simple liquid using the thermodynamics of the underlying hard-sphere fluid. This suggests

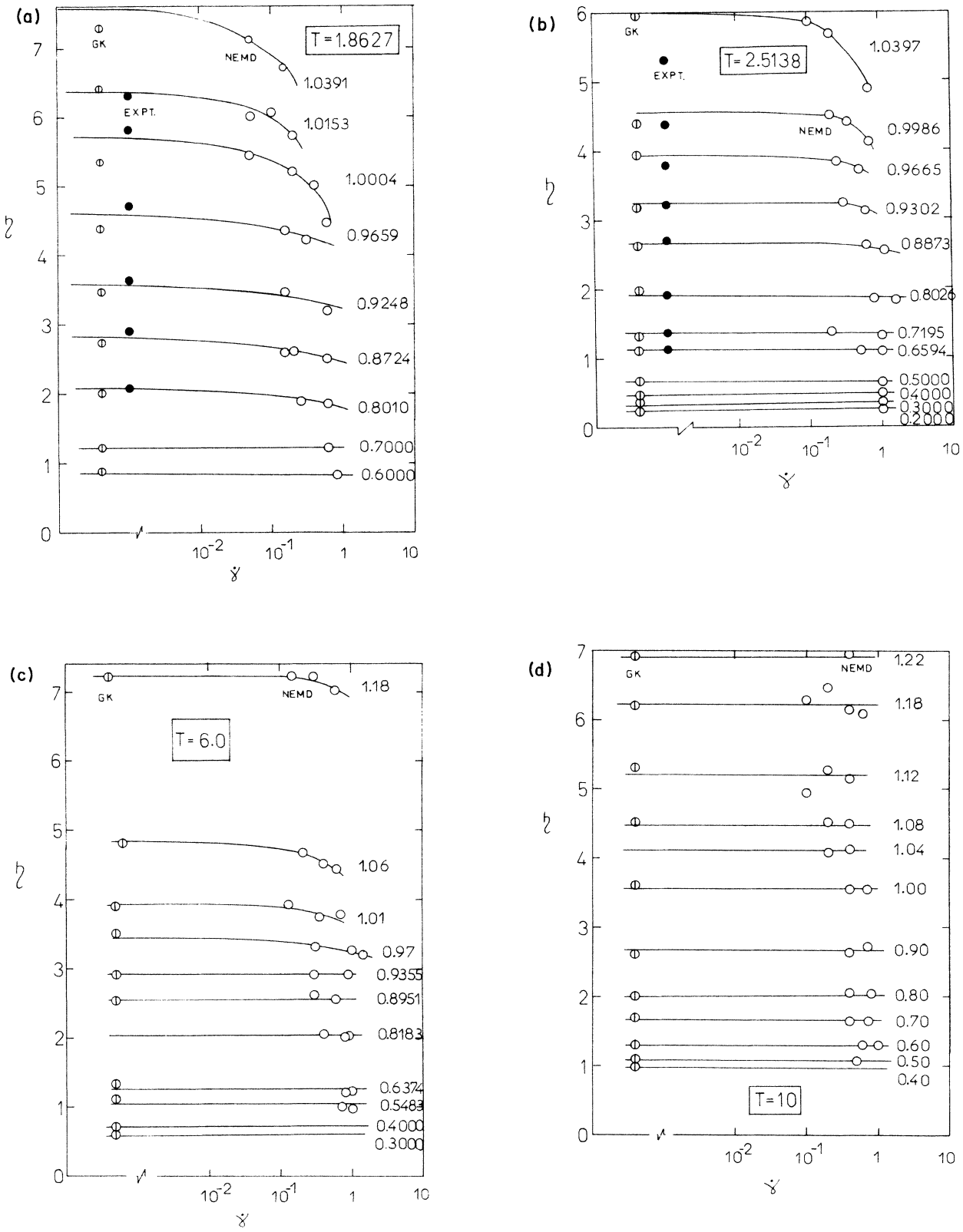

FIG. 1. Shear rate dependence of the LJ viscosity at densities along various isotherms. The reduced LJ number densities are indicated on the figure. Key: ⊕ are the largest N (EMD) values obtained from the Green-Kubo integral, Eq. (42), ● are experimental points for argon (Refs. 22 and 31). For argon, $m = 39.948 \times 10^{-3}$ kg mol^{-1}, $\varepsilon/k_B = 119.8$ K, and $\sigma = 0.3405$ nm. Interconversion factors from real to reduced units: $\rho^* = 23.78/(V_m/\text{cm}^3\text{mol}^{-1}) = 5.951 \times 10^{-4}\rho_m(\text{kg/m}^3)$, where V_m is the molar volume and ρ_m is the mass density. ○ are the values obtained by NEMD, $N = 256$. (a) $T^* = 1.8627$, (b) $T^* = 2.5138$, (c) $T^* = 6.0$, (d) $T^* = 10.0$.

that the hard-sphere fluid could be used as a reference fluid in interpreting the effects of temperature and pressure on the transport coefficients of more complicated nonassociated molecular fluids. The details of the model are described below.

Kinetic theory gives the TC of an infinitely dilute gas composed of hard spheres of mass m and diameter σ at temperature T.[22,23] These quantities for self-diffusion, D_0, shear viscosity, η_0, and thermal conductivity, λ_0, are

$$D_0=\frac{3}{8\rho_0^2}\left[\frac{k_BT}{\pi m}\right]^{1/2}, \tag{58}$$

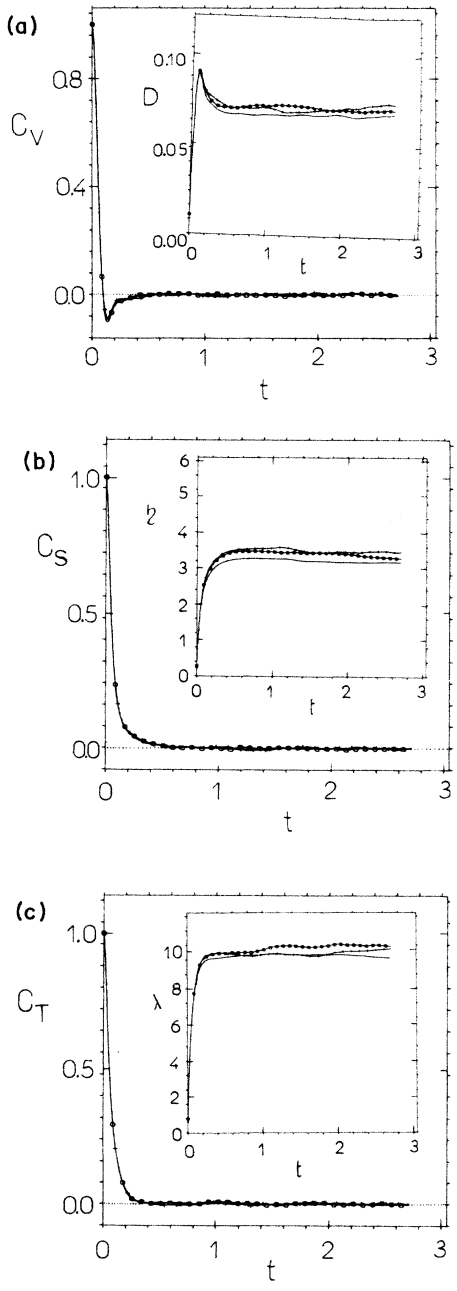

FIG. 2. The N dependence of the normalized time correlation functions and their integrals (shown as inserts) scaled using the Green-Kubo expressions of Eqs. (41), (42), and (45) to give the transport coefficients. $\rho=0.9248$ and $T=1.8627$. Key: $N=108$, ○ $N=256$, and + $N=500$. (a) The normalized [i.e., $C_V(0)=1$] velocity autocorrelation and self-diffusion coefficient, D. (b) The normalized shear stress autocorrelation function and shear viscosity, (c) heat flux autocorrelation function and thermal conductivity.

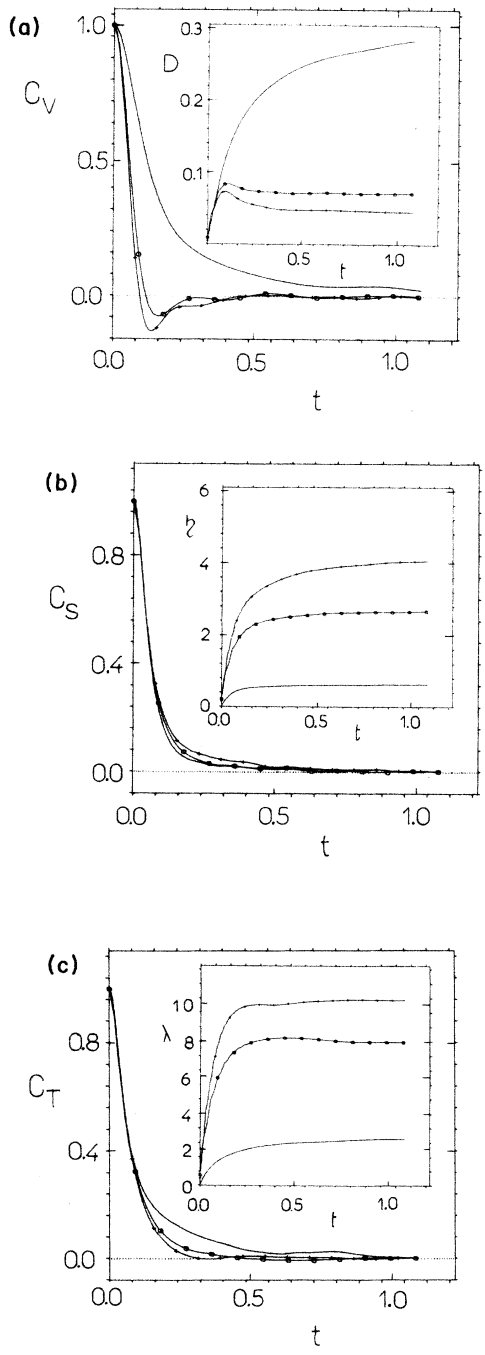

FIG. 3. Density dependence of (a) the normalized velocity autocorrelation function and self-diffusion coefficient, (b) the normalized shear stress autocorrelation function and shear viscosity, (c) the normalized heat current autocorrelation function and thermal conductivity, for the $T^*=1.4562$ isotherm. Key: —— $\rho=0.5249$, ○○○○ $\rho=0.8630$, and ++++ $\rho=0.938$; $N=256$.

$$\eta_0=\frac{5}{16\sigma^2}\left[\frac{mk_BT}{\pi}\right]^{1/2}, \tag{59}$$

and

$$\lambda_0=\frac{75}{64\sigma^2}\left[\frac{k_B^3T}{\pi m}\right]^{1/2}, \tag{60}$$

where k_B is the Boltzmann constant. The reduced density $\rho=(N/V)\sigma^3$, where N is the number of spheres in volume V. The Chapman-Enskog solution of the Boltzmann equation leads to density dependent self-diffusion coefficients, shear viscosities and thermal conductivities, which will be denoted by D_E, η_E, and λ_E, respectively.[24,25]

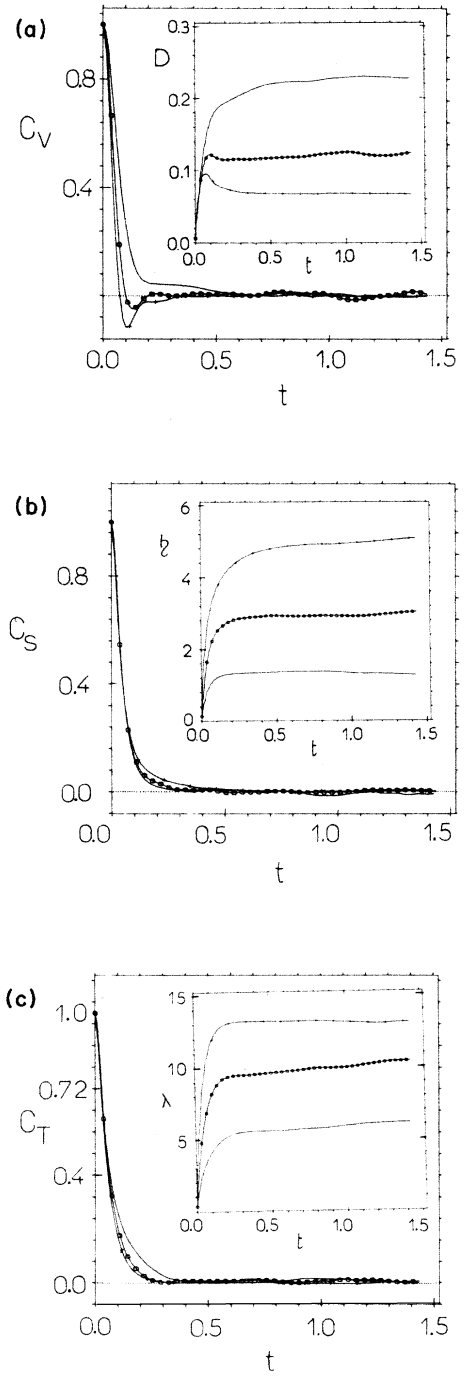

FIG. 4. As for Fig. 3 except that $T=2.5138$ and —— $\rho=0.7195$, ○○○○ $\rho=0.9094$, and ++++ $\rho=1.0135$; $N=256$.

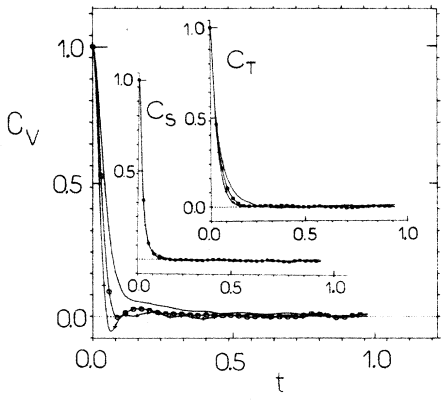

FIG. 5. The density dependence of the normalized time correlation functions for $T=10$ and —— $\rho=0.8$, ○○○○ $\rho=1.0$, and ++++ $\rho=1.18$; $N=256$.

$$\rho D_E/\rho D_0=\frac{1}{g(\sigma)}, \tag{61}$$

where $g(\sigma)$ is the value of the pair radial distribution function as contact of the spheres.

Similarly,

$$\frac{\eta_E}{\eta_0}=g(\sigma)^{-1}+0.8b\rho+0.7614g(\sigma)b^2\rho^2, \tag{62}$$

where $b=2\pi\sigma^3/3$, is the excluded volume in the van der Waals equation of state

$$\frac{\lambda_E}{\lambda_0}=g(\sigma)^{-1}+1.2b\rho+0.755g(\sigma)b^2\rho^2. \tag{63}$$

The equation of state of the hard-sphere fluid is related to $g(\sigma)$ through,

$$g(\sigma)=\left[\frac{PV}{Nk_BT}-1\right]\Big/\rho b, \tag{64}$$

where P is the pressure. A simple accurate equation of state of the hard sphere fluid has been recently derived,[26]

$$\frac{PV}{Nk_BT}=1+\frac{bv}{(v-v_0^1)^2}, \tag{65}$$

where

$$v=V/N. \tag{66}$$

The volume v_0^1 is used to define an effective free volume $v-v_0^1$. The value of v_0^1 is not known exactly because it can be considered to be an effective occupied volume. We can place bounds on it however and it lies somewhere between the close packed volume per particle, $v_0=\sigma^3/2^{1/2}$ and the volume of the sphere $(\pi/6)\sigma^3$. It is

convenient to define, $X=v/v_0$, $X_1=v/v_0^1$ where $X_1=fX$. The value of $f=1.1491$ gives good overall agreement with simulation data for the equation of state of the hard sphere fluid. Interestingly this is equivalent to a v_0 value half way between the designated bounds above. Substituting Eq. (65) in Eq. (64) gives an analytic expression for $g(\sigma)$ in terms of X_1 which can be used in Eqs. (61)–(63),

$$g(\sigma)=X_1^2/(1-X_1^2)\ . \tag{67}$$

Consequently,

$$\rho D_E/\rho D_0=(X_1-1)^2/X_1^2\ , \tag{68}$$

$$\eta_E/\eta_0=\frac{X_2^4+0.8CX_1X_2^2+0.7614C^2X_1^2}{X_1^2X_2^2}\ , \tag{69}$$

where $X_2=X_1-1$ and $C=2\pi 2^{1/2}f/3$.

$$\lambda_E/\lambda_0=\frac{X_2^4+1.2CX_1X_2^2+0.755C^2X_1^2}{X_1^2X_2^2}\ . \tag{70}$$

Hard-sphere MD calculations give essentially exact transport coefficients.[20–23] A comparison with the predictions of Eqs. (68)–(70) shows that these formulas agree with the simulations up to densities ~ 0.83 (or $v/v_0 \lesssim 1.7$). Above this density region (and at lower densities for D due to vortex flows) corrections to Eqs. (68)–(70) can be obtained. They are derived by parametrizing the hard sphere MD data. Consequently, for hard spheres

$$\rho D=\left[\frac{\rho D}{\rho D_E}\right]\left[\frac{\rho D_E}{\rho D_0}\right](\rho D_0)\ , \tag{71}$$

$$\eta=\left[\frac{\eta}{\eta E}\right]\left[\frac{\eta_E}{\eta_0}\right]\eta_0\ , \tag{72}$$

and

$$\lambda=\left[\frac{\lambda}{\lambda_E}\right]\left[\frac{\lambda_E}{\lambda_0}\right]\lambda_0\ . \tag{73}$$

Simulation gives,

$$\frac{\rho D}{\rho D_E}=a+b\rho+c\rho^2+d\rho^3+e\rho^4\ , \tag{74}$$

where $a=1.035$, $b=-0.553$, $c=5.640$, $d=-7.639$, and $e=1.814$. This is a fit to the available simulation data for hard spheres. Similarly for the shear viscosity, we use a literature expression,[22]

$$\frac{\eta}{\eta_E}=1.02+15(X^{-1}-0.35)^3+350(X^{-1}-0.575)^3 \qquad X^{-1}>0.575\ ,$$
$$=1.02+15(X^{-1}-0.35)^3 \quad 0.42<X^{-1}<0.575\ ,$$
$$=1.02 \quad X^{-1}<0.42\ . \tag{75}$$

Also, using literature values[21] for λ/λ_E we fit,

$$\frac{\lambda}{\lambda_E}=f+g\rho+h\rho^2+i\rho^3+j\rho^4\ , \tag{76}$$

where $f=0.990$, $g=0.160$, $h=-0.746$, $i=1.215$, and $j=-0.558$. Simplifications to Eqs. (71)–(73) were proposed by Dymond[23] over a limited region of $X(1.6\lesssim X\lesssim 2.5)$ as follows on rearrangement,

$$\frac{D_m^{1/2}}{k_B^{1/2}v_0^{1/3}T^{1/2}}=\frac{3}{8}\frac{1}{\pi^{1/2}}\frac{1.271}{2^{1/3}}(X-1.384)\ , \tag{77}$$

$$\frac{k_B^{1/2}m^{1/2}T^{1/2}}{v_0^{2/3}\eta}=2^{1/3}\pi^{1/2}\tfrac{16}{5}0.2195(X-1.384)\ , \tag{78}$$

$$\frac{k_B^{3/2}T^{1/2}}{m^{1/2}v_0^{2/3}\lambda}=2^{1/3}\pi^{1/2}\tfrac{64}{75}0.1611(X-1.217)\ , \tag{79}$$

Eq. (78) is a particularly good approximation to Eq. (72).

In order to apply the above formulas to the Lennard-Jones fluid an effective hard sphere diameter, σ, must be associated with each molecule. This is temperature dependent, but not density dependent to a good approximation. (As it is not density dependent it is not pressure dependent under isothermal conditions.) We use the fitting procedure of Dymond[27] to obtain $\sigma(T)$, which equates $\eta/\rho^{2/3}$ for the hard sphere and LJ systems and then uses the ratio of the two densities,

$$\sigma^*=\sigma/\sigma_{LJ}=(\rho/\rho_{LJ})^{1/3}\ , \tag{80}$$

where $\rho_{LJ}=(N/V)\sigma_{LJ}^3$ is the diameter in the Lennard-Jones potential. Van der Gulik and Trappeniers[28] have argued that at temperatures below and close to the critical temperature the effective hard-sphere diameter is different in the intermediate and high-density regimes. The attractive part of the LJ potential has a greater influence at high and very low densities (where it causes clusters at low temperature). At intermediate densities $(2\lesssim v/v_0\lesssim 4)$ the attractive component of the pair potential acts effectively as a uniform background, so that hard sphere behavior would be expected with an effective diameter which is not necessarily the same as that appropriate to the two density extremes. Assigning this regime as the most representative of "true" hard-sphere behavior it would suggest that a temperature independent effective hard-sphere diameter is required in D_0, η_0, and λ_0 (at least for $T\lesssim 2$). The LJ diameter has been found to be suitable for this.[28] This modification will be considered in the discussion.

Dymond reductions of Eqs. (68)–(70) are different to Eqs. (77)–(79) with this choice of intermediate density hard-sphere diameter (i.e., $\sigma=\sigma_{LJ}$) for D_0, η_0, and λ_0. This modification gives

$$\frac{Dm^{1/2}}{k_B^{1/2}T^{1/2}V_0}=\frac{3}{8}\frac{1.271}{\pi^{1/2}}(X-1.384)\ , \tag{81}$$

$$\frac{k_B^{1/2}m^{1/2}T^{1/2}}{\eta}=\tfrac{16}{5}\pi^{1/2}0.2195(X-1.384)\ , \tag{82}$$

and

$$\frac{k_B^{1/2}T^{1/2}}{m^{1/2}\lambda}=\tfrac{64}{75}\pi^{1/2}0.1611(X-1.217)\ . \tag{83}$$

There is much current interest in the temperature and pressure dependence of transport coefficients. Using an

Arrhenius form we can ensure compliance with experimental data by adopting a temperature and density dependent activation energy and volume. These are defined in

$$A(T)=A_0\exp[E_a(\rho,T)/k_BT]\ , \tag{84}$$

$$A(P)=A_0\exp(\alpha P)\ , \tag{85}$$

where $A=D^{-1}$, η or λ. E_a is an activation energy. Also,

$$V_a(T,\rho)=\alpha(T,\rho)k_BT\ , \tag{86}$$

where V_a is an activation volume.

This treatment is applied even though single-particle motion in a simple liquid is clearly not a simple or "Arrhenius" activated process.[29,30] Therefore these equations have no obvious mechanistic foundation but do provide a definition of "effective" activation energies and volumes, which are nevertheless very useful in appreciating trends. By definition,

$$E_V/k_B=[\partial(\ln A)/\partial(1/T)]_V\ , \tag{87}$$

$$E_P/k_B=[\partial(\ln A)/\partial(1/T)]_P\ , \tag{88}$$

the constant volume and constant pressure activation energies, respectively. Also by definition,

$$\alpha=[\partial(\ln A)/\partial P]_T\ . \tag{89}$$

As,

$$\left[\frac{\partial\ln A}{\partial T}\right]_V=\left[\frac{\partial\ln A}{\partial T}\right]_P+\left[\frac{\partial\ln A}{\partial P}\right]_T\left[\frac{\partial P}{\partial T}\right]_V\ , \tag{90}$$

then,

$$E_V=E_P-k_BT^2\propto\left[\frac{\partial P}{\partial T}\right]_V\ . \tag{91}$$

If the LJ molecules can be represented by a density independent effective hard sphere diameter $\sigma(T)$ then

$$\left[\frac{\partial\ln A}{\partial T}\right]_{X_1}\quad\text{and}\quad\left[\frac{\partial\ln A}{\partial X_1}\right]_T\ ,$$

for the LJ fluid can be equated to that of the hard-sphere fluid, which are known analytically. By definition,

$$\left[\frac{\partial\ln A}{\partial T}\right]_V=\left[\frac{\partial\ln A}{\partial T}\right]_{X_1}-\beta_0X_1\left[\frac{\partial\ln A}{\partial X_1}\right]_T\ , \tag{92}$$

where

$$\beta_0=\left[\frac{dV_0}{dT}\right]\Big/V_0=3\left[\frac{d\sigma}{dT}\right]\Big/\sigma \tag{93}$$

is the expansivity of the close-packed volume and $V_0=Nv_0$. Hence, using Eq. (49) in Eq. (44),

$$\frac{E_V}{k_BT}=-T\left[\left[\frac{\partial\ln A}{\partial T}\right]_{X_1}-\beta_0X_1\left[\frac{\partial\ln A}{\partial X_1}\right]_T\right]\ . \tag{94}$$

Therefore E_V for the LJ fluid has been written analytically in terms of the transport coefficients A of the hard sphere fluid and a thermodynamic property of the LJ fluid, β_0. A similar expression for E_P can be derived as follows

$$\left[\frac{\partial\ln A}{\partial T}\right]_P=\left[\frac{\partial\ln A}{\partial T}\right]_{X_1}+\left[\frac{\partial\ln A}{\partial X_1}\right]_T\left[\frac{\partial X_1}{\partial T}\right]_P\ . \tag{95}$$

Now,

$$\left[\frac{\partial X_1}{\partial T}\right]_P=\left[\frac{\partial X_1}{\partial T}\right]_V+\left[\frac{\partial X_1}{\partial V}\right]_T\left[\frac{\partial V}{\partial T}\right]_P$$

$$=X_1(\beta-\beta_0)\ , \tag{96}$$

where the expansivity of the LJ fluid, β, is

$$\beta=\left[\frac{\partial V}{\partial T}\right]_P\Big/V\ . \tag{97}$$

Substituting Eq. (96) in Eq. (95) and using Eq. (88) we obtain

$$\frac{E_P}{k_BT}=-T\left[\left[\frac{\partial\ln A}{\partial T}\right]_{X_1}+(\beta-\beta_0)X_1\left[\frac{\partial\ln A}{\partial X_1}\right]_T\right]\ . \tag{98}$$

As

$$\left[\frac{\partial\ln A}{\partial T}\right]_{X_1}>0\ \text{and}\ \left[\frac{\partial\ln A}{\partial X_1}\right]_T<0\ ,$$

we can conclude that $E_P\geq E_V$ for all LJ state points.

The difference between the constant pressure and volume activation energies follows from Eqs. (94) and (98)

$$E_P-E_V=-k_BT^2\beta X_1\left[\frac{\partial\ln A}{\partial X_1}\right]_T\ . \tag{99}$$

The pressure transport coefficient α can also be related to a hard-sphere fluid which has the same transport coefficients as the LJ fluid. Again a second-order thermodynamic quantity of the LJ fluid is required as follows. Equations (91) and (99) give

$$\alpha=-\beta X_1\left[\frac{\partial\ln A}{\partial X_1}\right]_T\Big/\left[\frac{\partial P}{\partial T}\right]_V\ ,$$

$$=-\kappa X_1\left[\frac{\partial\ln A}{\partial X_1}\right]_T\ , \tag{100}$$

where κ is the isothermal compressibility,

$$\kappa=-\left[\frac{\partial V}{\partial P}\right]_T\Big/V\ . \tag{101}$$

It remains to evaluate $(\partial\ln A/\partial X_1)$ and $(\partial\ln A/\partial T)_{X_1}$ for hard sphere $A=D^{-1}$, η, and λ. These quantities for the analytic representations of the hard-sphere transport coefficients are given below. Let $\rho D_{E0}=\rho D_E/\rho D_0$ and $\rho D_{E1}=\rho D/\rho D_E$. Then

$$\left[\frac{\partial \ln D}{\partial X_1}\right]_T = \rho D_0(\rho D_{E0}\rho D_2 + \rho D_1 \rho D_{E1})/\rho D \ , \tag{102}$$

where

$$\rho D_{E0} = (X_1-1)^2/X_1^2 \ , \tag{103}$$

$$\rho D_1 = \frac{d(\rho D_{E0})}{dX_1} = \frac{2(X_1-1)}{X_1^2} - \frac{2(X_1-1)^2}{X_1^3} \ , \tag{104}$$

and

$$\rho D_2 = \frac{d(\rho D_{E1})}{dX_1} = -\frac{\rho}{X_1}(b + 2c\rho + 3d\rho^2 + 4e\rho^3) \ . \tag{105}$$

Similarly for shear viscosity, let $\eta_{E0} = \eta_E/\eta_0$ and $\eta_{E1} = \eta/\eta_E$ from Eq. (75). Then,

$$\left[\frac{\partial \ln \eta}{\partial X_1}\right] = \eta_0(\eta_{E0}\eta_2 + \eta_1\eta_{E1})/\eta \ , \tag{106}$$

where

$$\eta_{E0} = \frac{(X_1-1)^2}{X_1^2} + \frac{A}{X_1} + \frac{B}{(X_1-1)^2} \ , \tag{107}$$

where $A = 0.8C$, $B = 0.7614C^2$, and $C = 2\pi 2^{1/2} f/3$

$$\eta_1 = \frac{d(\eta_{E0})}{dX_1} = \frac{2(X_1-1)}{X_1^2} - \frac{2(X_1-1)^2}{X_1^3} - \frac{A}{X_1^2} - \frac{2B}{(X_1-1)^3} \ , \tag{108}$$

$$\eta_2 = \frac{d(\eta_{E1})}{dX_1}$$

$$= [-45(X^{-1}-0.35)^2/X^2 - 1050(X^{-1}-0.575)^2/X^2]/f \quad X^{-1} > 0.575$$

$$= [-45(X^{-1}-0.35)^2/X^2]/f \quad 0.42 < X^{-1} < 0.575$$

$$= 0 \quad X^{-1} < 0.42 \ . \tag{109}$$

Analogous expressions exist for thermal conductivity, if $\lambda_{E1} = \lambda/\lambda_E$ from Eq. (76) then,

$$\left[\frac{\partial \ln \lambda}{\partial X_1}\right]_T = \lambda_0(\lambda_{E0}\lambda_2 + \lambda_1\lambda_{E1})/\lambda \ , \tag{110}$$

$$\lambda_{E0} = \frac{(X_1-1)^2}{X_1^2} + \frac{D}{X_1} + \frac{E}{(X_1-1)^2} \ , \tag{111}$$

where $D = 1.2\ C$ and $E = 0.755\ C^2$

$$\lambda_1 = \frac{d(\lambda_{E0})}{dX_1} = \frac{2(X_1-1)}{X_1^2} - \frac{2(X_1-1)^2}{X_1^3} - \frac{D}{X_1^2} - \frac{2E}{(X_1-1)^3} \ , \tag{112}$$

$$\lambda_2 = \frac{d(\lambda_{E1})}{dX_1} = -\frac{\rho}{X_1}(g + 2h\rho + 3i\rho^2 + 4j\rho^3) \ , \tag{113}$$

where g, h, i, and j are those defined for Eq. (76). For all three transport coefficients,

$$\left[\frac{\partial \ln A}{\partial T}\right]_{X_1} = \tfrac{1}{2}T \ . \tag{114}$$

The next step is to substitute Eqs. (102), (106), (110), and (114) into the expressions for the LJ E_V, E_P, and α, in Eqs. (94), (98), and (100), respectively. An alternative procedure which leads to simpler expressions for the LJ E_V, E_P, and α result from the linear fits to D, η^{-1}, and λ^{-1} given in Eqs. (77)–(79) or Eqs. (81)–(83). The difference between these two series of equations is in the choice for the hard-sphere diameter in ρD_0, η_0, and λ_0. For self-diffusion using Eq. (77) in Eqs. (94), (98), and (100), respectively,

$$\frac{E_V}{k_B T} = \tfrac{1}{2} - \beta_0 T\left[\frac{X}{X-1.384} - \frac{1}{3}\right] \ , \tag{115}$$

$$\frac{E_P}{k_B T} = \tfrac{1}{2} - (\beta_0 - \beta)\frac{TX}{X-1.384} + \frac{\beta_0 T}{3} \ , \tag{116}$$

$$\alpha = \frac{X}{(X-1.384)}\kappa \ . \tag{117}$$

Also for shear viscosity and thermal conductivity,

$$\frac{E_V}{k_B T} = -\tfrac{1}{2} - \beta_0 T\left[\frac{X}{X-y} - \frac{2}{3}\right] \ , \tag{118}$$

$$\frac{E_P}{k_B T} = -\tfrac{1}{2} - (\beta_0 - \beta)\frac{TX}{X-y} + \tfrac{2}{3}\beta_0 T \ , \tag{119}$$

$$\alpha = \frac{X}{(X-y)}\kappa \ , \tag{120}$$

and $y = 1.384$ for η and $y = 1.217$ for λ.

The corresponding relationships from Eqs. (81)–(83) are, for self-diffusion,

$$\frac{E_V}{k_B T} = \tfrac{1}{2} - \beta_0 T\left[\frac{X}{X-1.384} - 1\right] \ , \tag{121}$$

$$\frac{E_P}{k_B T}=\tfrac{1}{2}-(\beta_0-\beta)\frac{TX}{X-1.384}+\beta_0 T\ , \tag{122}$$

and

$$\alpha=\frac{X}{X-1.384}\kappa\ . \tag{123}$$

Also for η and λ,

$$\frac{E_V}{k_B T}=-\tfrac{1}{2}-\beta_0 T\frac{X}{(X-y)}\ , \tag{124}$$

$$\frac{E_P}{k_B T}=-\tfrac{1}{2}-(\beta_0-\beta)\frac{TX}{(X-y)}\ , \tag{125}$$

and

$$\alpha=\frac{X}{(X-y)}\kappa\ . \tag{126}$$

With the simple expressions of (116)–(126) we relate LJ "second-order transport coefficients" [e.g., $(\partial \ln\eta/\partial T)_V$] through E_V, E_P, and α to LJ second-order thermodynamic quantities, β_0, β, and κ. This is made through the intermediary of the hard-sphere equation of state and its density (and temperature) dependent transport coefficients.

The temperature-dependent effective hard-sphere diameter for the LJ molecules was obtained using the Dymond matching procedure[27] applied to the shear viscosities. The values obtained are presented in Table II. We obtain also by a least squares fit to this data,

$$\sigma_{\rm HS}/\sigma_{\rm LJ}=a_1+a_2T+a_3T^2+a_4T^3+a_5T^4\ , \tag{127}$$

where $a_1=1.1726$, $a_2=-0.360\,99$, $a_3=0.281\,74$, $a_4=-0.109\,02$, and $a_5=0.0159\,53$, on assuming that the hard sphere diameter equals the LJ diameter in ρD_0, η_0, and λ_0 and that $T\lesssim 2.5$. Alternatively, $a_1=1.095\,59$, $a_2=-0.122\,135$, $a_3=0.034\,084$, $a_4=-0.004\,56$, and $a_5=0.000\,212\,35$, on taking the dense fluid hard-sphere diameter to apply also for the dilute gas transport coefficients and that $T\lesssim 10.0$.

TABLE II. The temperature-dependent effective hard-sphere diameters in the LJ reduced unit of distance, according to *A*, the Gulik *et al.* method used in Eqs. (81), (82), (83), and (121)–(126). *B* applying the high-density effective diameter at all densities and leading to Eqs. (77)–(79), and Eqs. (115)–(120).

T	*A* $\sigma_{\rm HS}/\sigma_{\rm LJ}$	*B* $\sigma_{\rm HS}/\sigma_{\rm LJ}$
0.72	1.0219	1.0226
0.81	1.0151	1.0171
1.0	1.000	1.005
1.06	0.9939	0.9946
1.2	0.994	1.000
1.35	0.9817	0.9794
1.4562	0.9794	0.9743
1.8627	0.9653	0.9580
2.5138	0.9508	0.9396
2.6974	0.9477	0.9360
3.5	0.935	0.925
4.5	0.915	0.905
6.0	0.90	0.880
10.0		0.8433

VI. TEST OF THE EFFECTIVE HARD-SPHERE MODEL

In this section, the hard-sphere model described in Sec. V is applied to the data of Table I, using the effective diameters given in Table II for the LJ fluids and parametrized in Eq. (127). First we consider the extent to which the simulation data adheres to Eqs. (71)–(73), for the exact hard-sphere transport coefficients, and the Dymond simplifications given in Eqs. (77)–(79).

First, the viscosity of the LJ fluid reduced according to Eq. (78) is compared with the linear relationship in V/V_0 from that equation (B) and that derived from the more exact representation for the hard-sphere viscosity, Eq. (72). In Fig. 6 it is seen that, over the temperature range considered both expressions reproduce the LJ shear viscosity within simulation uncertainties.

The linear relationship in V/V_0 is probably good enough for most practical applications of this hard sphere based representation of the LJ viscosity. There is a relatively minor trend for the hard sphere approach to over estimate the viscosity for lower densities ($\rho\approx 0.6-0.7$ at $T\lesssim 3$). We attribute this to "clustering" phenomena arising from the attractive part of the potential. This feature is not apparent at higher temperatures, at which the attractive part of the potential has a less influential role in determining the molecular dynamics. In Fig. 6(d) an example is considered of the proposed viscosity reduction, which is implicit in van der Gulik *et al.* adoption of a variable hard-sphere diameter for the terms in Eq. (72). The relevant equations for curves *B* and *A* are Eq. (82) and Eq. (72). Comparison with Fig. 6(a) reveals that there is little improvement for the data and this approach would appear to be an unnecessary complication for the purposes of this work.

In Fig. 7 the corresponding curves for self-diffusion are considered, Eqs. (77) and (71), and Eq. (81) for the van der Gulik *et al.* method. Apart from temperatures below about 1.35 and (therefore) close to the solid phase boundary it is not possible to predict both self-diffusion coefficients and the shear viscosity using the same effective hard sphere diameter. The self-diffusion coefficient obtained by LJ simulation is less than the prediction of the hard-sphere lines *A* and *B*. Again this could be partly due to "clustering" caused by the attractive part of the potential. However, there must be another source of this discrepancy because the extent of agreement with the hard sphere curves *decreases* with increasing temperature. The influence of pair, triplet. . . associations of molecules would be expected to diminish as the temperature increases. It could be argued that it is by using the viscosity in the Dymond fitting procedure, that the fit is inevitably better for viscosity than self-diffusion. However, this does not explain the good simultaneous fits at high density and low temperature. Also, the thermal conductivity curves [Eqs. (73), (79), and (83)] in Fig. 8 reveal an excellent agreement with the hard sphere predictions at high temperature, using the same effective hard-

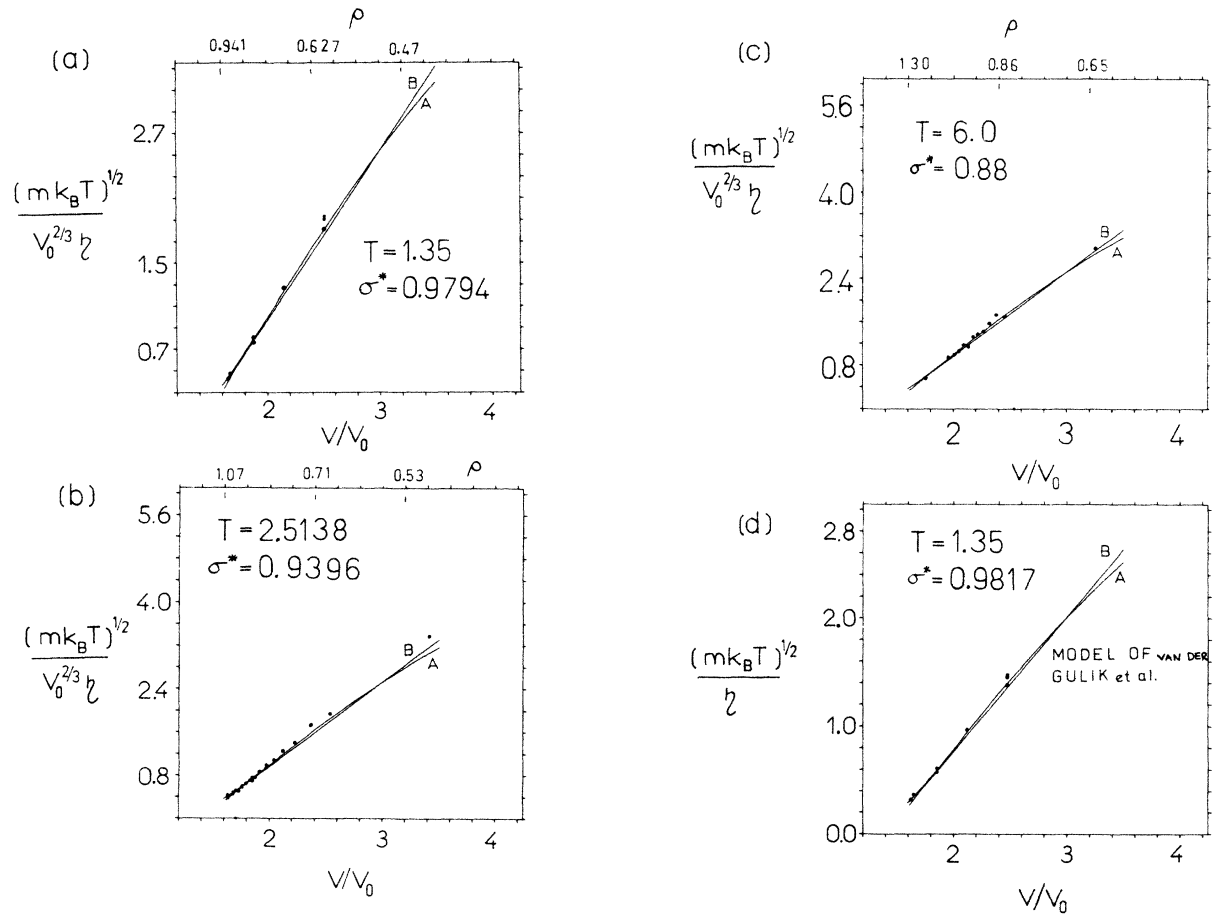

FIG. 6. Reductions of the shear fluidity as suggested by Dymond (Ref. 23) and given in Eq. (78) (a) $T^*=1.35$, $\sigma^*=\sigma_{HS}/\sigma_{LJ}=0.9794$, (b) $T^*=2.5138$, $\sigma^*=0.9396$, (c) $T^*=6.0$, $\sigma^*=0.88$ for the temperature dependent σ^* employed in η_0. (d) $T^*=1.35$ and $\sigma^*=0.9817$ for $\sigma^*=1.0$ employed in η_0, Eq. (82). Curve A is derived from Eq. (72). Curve B is from Eq. (78).

sphere diameters as for the viscosity. [Again, the modification proposed by van der Gulik *et al.* would appear to be unnecessary here, and an overcomplicating feature.] In this case there is an overestimation of the thermal conductivity at low temperature by the hard-sphere approach. This one would expect intuitively. The attractive part of the potential acts as a heat sink and hinders fast heat flux transfer. This extra property of the fluid, which is not exhibited by the "corresponding" hard-sphere fluid, becomes less important at high temperature. The pattern established is therefore as follows. The properties of the hard sphere fluid account well for the viscosity at all temperatures and densities (at least above about half the maximum fluid density at any particular temperature and also where a density is not excluded by being in the two phase region, i.e., at $T^* \lesssim 1.3$). This model is also useful for self-diffusion below $T=1.35$ for fluid states on the fluid-crystal boundary. At lower densities, and at higher temperatures at all densities, the self-diffusion coefficient is seriously overestimated by the hard-sphere model. This is presumably a consequence of the softness of the pair potential. Figure 5 presents supporting evidence for this. There is a dramatic effect of density on the form of the velocity autocorrelation function for hard spheres. It exhibits a hydrodynamic long time tail at intermediate densities, and a negative "backscattering" lobe at higher densities. These are incompatible with the Enskog formulas, which have an underlying exponential time decay for all the dynamical processes. Although this deviation from the hard-sphere model dynamics is partially masked through the MD parametrized $(\rho D/\rho D_E)$ term in Eq. (71), this information does clearly illustrate the inadequacy of such a model to describe the true dynamics of single particles in a hard-sphere fluid at densities of interest here. The shear stress and heat current autocorrelation functions, in contrast, stay positive in the hard-sphere simulations. These correlation functions are therefore more similar to the assumed exponential time decay for dynamical processes in the Enskog theory. The poor account of single-particle motion must cancel out when many-body functions are evaluated. The LJ stress and heat current autocorrelation functions are also positive at all times, as revealed in Fig. 5. Therefore any deviation from a hard-sphere potential caused by a softening of the repulsive core, or by the addition of an attractive bowl to the potential, is likely to have a greater effect on the self-diffusion coefficient than on the shear viscosity or the thermal conductivity. This

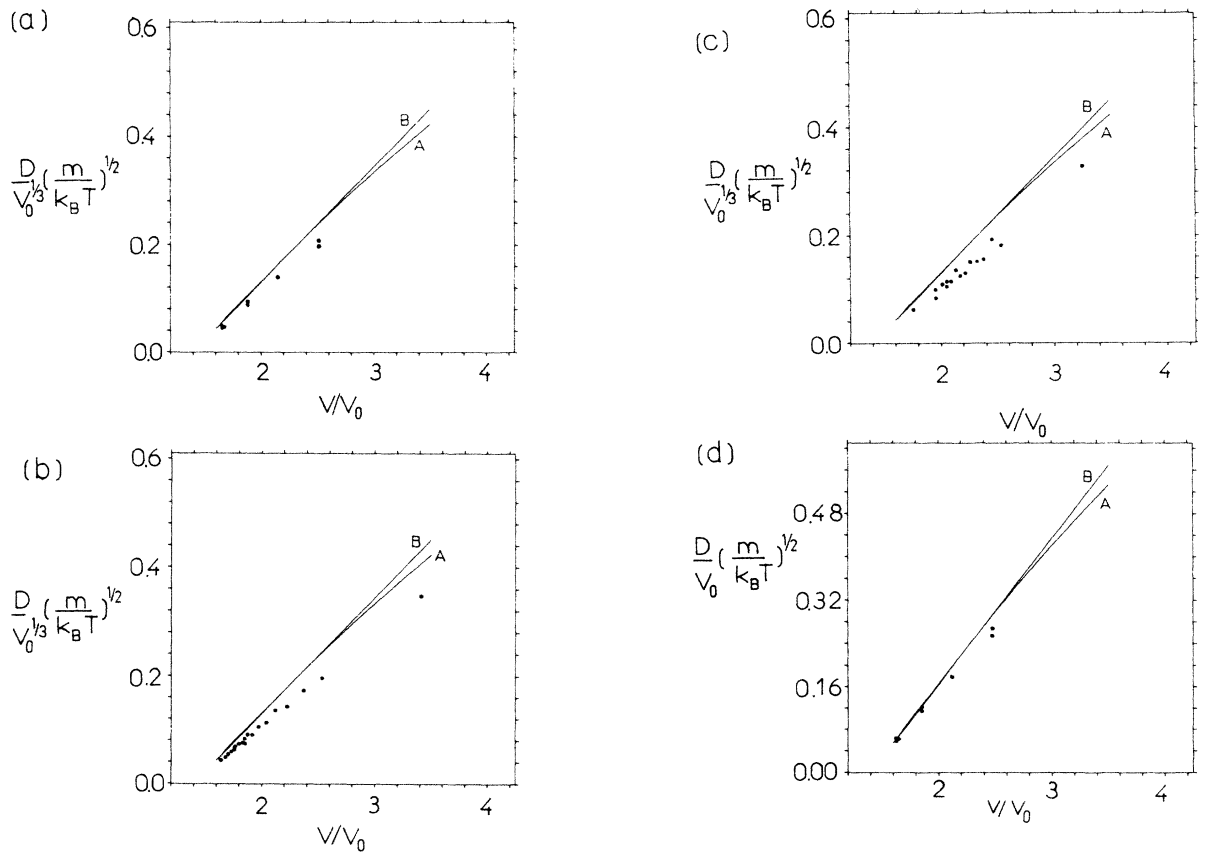

FIG. 7. As for Fig. 6 except that the self-diffusion coefficients are considered [Eq. (77) and (81)]. Curve *A* is derived from Eq. (71) and curve *B* is from Eq. (77).

is observed from Fig. 7. The agreement with the hard-sphere model *decreases* with increasing temperature. In contrast for thermal conductivity, the agreement improves with increasing temperature. The softening of the repulsive core is not an important factor for η or λ but for λ at low temperature the potential's attractive bowl is an important factor in diminishing the efficiency of heat transfer, and therefore reducing λ when compared with that of hard spheres.[33]

There have been many MD studies that have investigated the effect of adding an attractive component to a repulsive intermolecular potential. These include comparisons between repulsive and full LJ potentials,[33–36] and hard sphere and attractive square well molecules.[37–40] These two system pairs give the same qualitative behavior. Below the critical density and at low temperature, the attractive bowl to the potential can significantly decrease the self-diffusion coefficient below that of the repulsive reference fluid. Above the critical density the same trend is evident but becomes less pronounced as density increases to the solid transition.[33,40] In contrast, the behavior of the shear viscosity and thermal conductivity shows little change on the addition of an attractive component below the critical density. For the viscosity the square well fluid manifests a gradual increase towards the solid transition but this is very sensitive to the width of the bowl.[39] The thermal conductivity exhibits a more modest decrease at low temperature and high density.[38] These trends are in excellent agreement with the present work. It is worth noting that the most important deviations from hard-sphere behavior occur at densities lower than of interest for this work.

Now that the usefulness of a hard-sphere model for, in particular, shear viscosity has been demonstrated we consider the activation energies and volumes (from the pressure transport coefficients) that are analytically known from Eqs. (94), (98), (100), and (115)–(126).

We will consider the shear viscosity only, although the same treatments could be made for D and λ, but with less justification. Figure 9 presents the density dependence of the constant volume and constant pressure activation energies, E_V and E_P, for the $T^*=2$ LJ isotherm. (We use the temperature-dependent effective hard-sphere diameter in η_0.) This figure reveals that E_V is essentially zero or negative for densities below 0.8. The viscosity increases with temperature up to $\rho^*=0.7$, indicating that the residual properties of the dilute gas are dominating the shear viscosity up to quite high densities. In comparison, the E_P are substantially positive over the entire fluid range. The origin of this difference comes from the expansion of the fluid with increasing temperature. This tends to reduce the viscosity and overrides the kinetic component to E_P, which would tend to cause an increase in η with temperature. Figure 9 reveals also that the "ex-

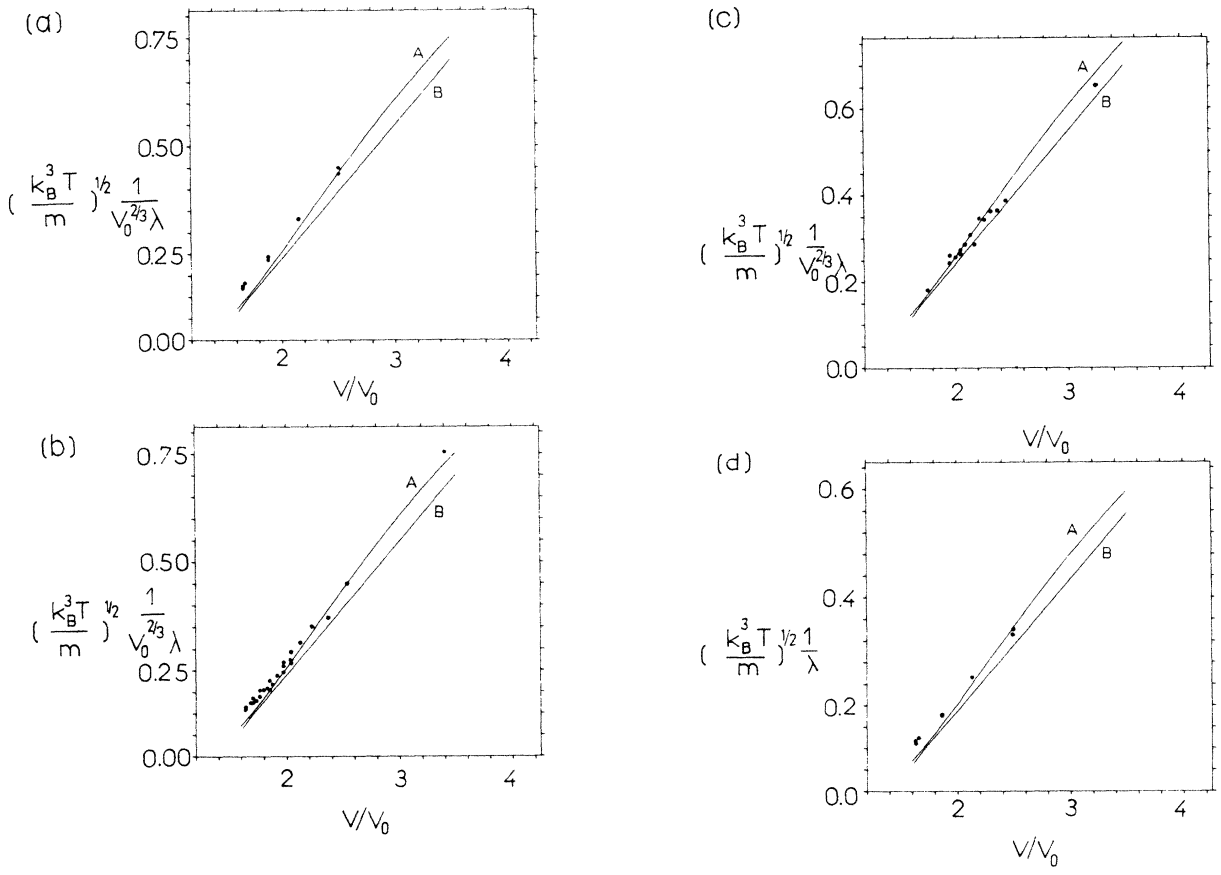

FIG. 8. As for Fig. 6 except that the thermal conductivity is considered. The relevant equations are Eqs. (73), (79), and (83).

act" expression for E_P and E_V in Eqs. (98) and (94), agrees reasonably well with the Dymond simplifications of Eqs. (119) and (118) and vindicates these simplified expressions for E_P and E_V. They could be made use of for other quasispherical molecular fluids.

The activation volume V_a curve along the same isotherm is presented in Fig. 10. The activation volume per molecule diminishes from 1 to 0.2 over the density range 0.5–1.0 This is consistent with the transition from a communally accessible volume for a molecule to a local "free" volume as the liquid approaches close packing. It is interesting to note that both E_V and E_P are negative over the entire fluid range at $T^*=10.0$ indicating the dominance of the purely kinetic component to the activation energies. The limit of V_a at high density ($\rho^*=1.1$) is 0.1. This reflects the closer approach of the LJ molecules (effectively soft spheres here) at this supercritical temperature. In Fig. 11 we compare E_V at $T=1.0$ given by Eqs. (94), (115), and (118). The Eq. (115) route, along the lines suggested by the van der Gulik *et al.* treatment,[28] is in satisfactory agreement with the more exact route of Eqs. (94) and (118) adopting the high density $\sigma(T)$ in the expression for η_0. This additional feature to the Enskog formulation is therefore of no significant advantage to satisfy the objectives of this work.

VII. CONCLUSIONS

It has been demonstrated that for simple fluids the methods of equilibrium and nonequilibrium molecular dynamics are practical alternatives to experiment in ob-

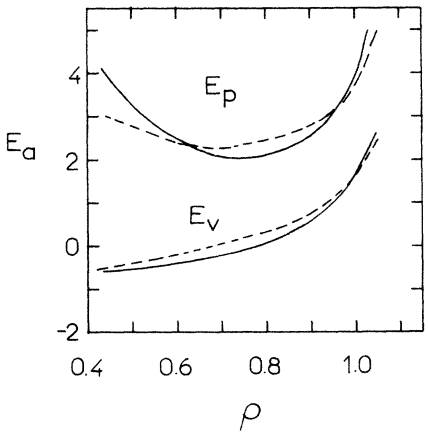

FIG. 9. Constant pressure and volume shear viscosity activation energies, E_P and E_V for a $T=2$ LJ isotherm are given. They are produced from for E_V: Eqs. (94) and (72) (----), the "exact" expressions and Eq. (118). For E_P: Eq. (98) and Eq. (119) (——).

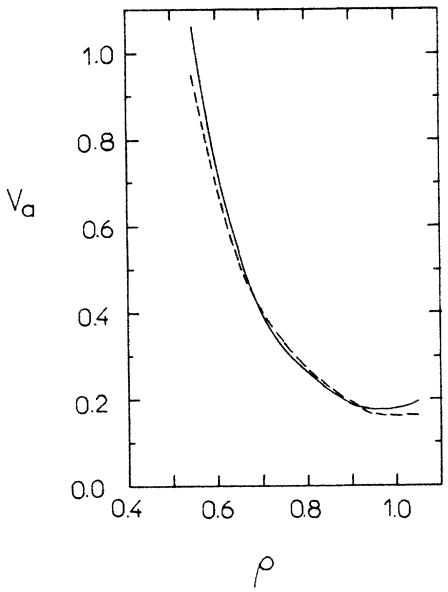

FIG. 10. As for Fig. 9 except that the activation volume V_a given by Eqs. (86) and (100) are considered. The relevant equations are, for the "exact" solution Eqs. (72), (100), and (106) (----). For the Dymond reduction Eq. (120) is used.

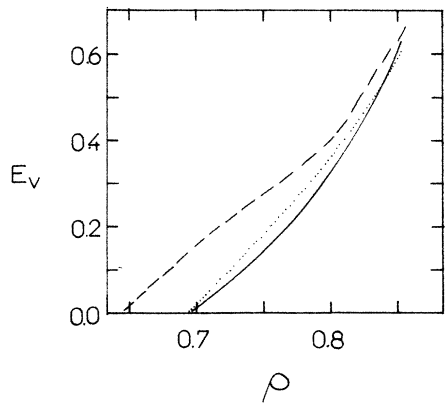

FIG. 11. The constant volume shear viscosity isotherms for E_V at $T=1.0$ using the "exact" model Eqs. (72), (94), (106), and (114) (----). For the Dymond reduction, $\sigma^*=1$ in η_0 (. . .) Eq. (124) and for $\sigma^*(T)$ in η (——) Eq. (118) was used.

taining transport coefficients. The results from these calculations are that, using accepted values for the LJ parameters to represent argon, the viscosities computed agree within similar statistical uncertainties with experiment across the fluid range. These viscosities, self-diffusion coefficients and thermal conductivities obtained by the Green-Kubo method were analyzed in terms of a MD modified Chapman-Enskog formulation for the hard-sphere fluid transport coefficients. A temperature-dependent effective hard-sphere diameter enables us to identify an arbitrary LJ state with its equivalent hard sphere fluid. Therefore one can predict the transport coefficients of the LJ fluid from its thermodynamic behavior. The application of this approach showed that the MD shear viscosity agrees well with the model predictions over all the fluid range above a density exceeding half the solidification density. The thermal conductivity had the next best overall agreement, differing only significantly at high density and low density. The self-diffusion coefficients were far from satisfactory in this respect, showing only adequate agreement at low temperature and high density. The deviations from hard sphere behavior are attributed to the attractive part of the potential and the softness of the repulsive core, in the latter case.

ACKNOWLEDGMENTS

The author thanks the Royal Society for the award of a Royal Society 1983 University Research Fellowship. Dr. D. MacGowan (BP Research Sunbury-on-Thames, United Kingdom) is thanked for helpful discussions. The University of London Computer Center is thanked for a generous allocation of CRAY-1S and AMDAHL 470-V/8 computer time.

[1]D. M. Heyes, J. Chem. Soc., Faraday Trans. 2, **79**, 1741 (1983).
[2]D. M. Heyes, J. Chem. Soc., Faraday Trans. 2, **80**, 1363 (1984).
[3]D. M. Heyes, J. Chem. Soc., Faraday Trans. 2, **82**, 1365 (1986).
[4]D. M. Heyes, J. Chem. Phys. **85**, 997 (1986).
[5]D. M. Heyes, Mol. Phys. **57**, 1265 (1986).
[6]Private communication, D. MacGowan, CCP5 Information Quarterly for Computer Simulation of Condensed Phases, 1986, No. 20, p. 32; supplied by the Science and Engineering Research Counsel Daresbury Laboratory, Daresbury, Warrington WA4 4AD, United Kingdom.
[7]D. J. Evans and G. P. Morriss, Phys. Rev. A **30**, 1528 (1984).
[8]J.-P. Hansen and I. R. McDonald, *Theory of Simple Liquids* (Academic, London, 1976).
[9]D. J. Evans and G. P. Morriss, Comput. Phys. Rep. **1**, 297 (1984).
[10]D. MacGowan (private communication).
[11]D. Levesque, L. Verlet, and J. Kurkijarvi, Phys. Rev. A **7**, 1690 (1973).
[12]D. MacGowan and D. J. Evans, Phys. Lett. **117A**, 414 (1986).
[13]S. K. Schiferl and D. C. Wallace, J. Chem. Phys. **83**, 5203 (1985).
[14]D. Fincham, Comput. Phys. Commun. **40**, 263 (1986).
[15]Private communication, M. J. Gillan, CCP5 Information Quarterly for Computer Simulation of Condensed Phases, 1985, No. 16, p. 82; an unrefereed informal newsletter supplied by the Science and Engineering Research Counsel Daresbury Laboratory, Daresbury, Warrington WA4 4AD, United Kingdom.
[16]J. van der Elsken and D. M. Heyes, Can. J. Phys. **59**, 1532 (1981).
[17]D. Frenkel, *Intermolecular Spectroscopy and Dynamical Properties of Dense Systems* (Society of Italiana di Fisica, Bologna,

1980) pp. 156-201.
[18]M. G. Kim, J. Korean Phys. Co. **16**, 165 (1983).
[19]J. Jäckle, Rep. Prog. Phys. **49**, 171 (1986).
[20]A. J. Easteal, L. A. Woolf, and D. L. Jolly, Physica **121A**, 286 (1983).
[21]J. J. Erpenbeck and W. W. Wood, Phys. Rev. A **32**, 412, (1985).
[22]P. S. van der Gulik and N. J. Trappeniers, Physica **135A**, 1 (1986).
[23]J. H. Dymond, J. Chem. Phys. **60**, 969 (1974).
[24]J. O. Hirschfelder, C. F. Curtis, and R. B. Bird, *Molecular Theory of Gases and Liquids* (Wiley, New York, 1954).
[25]D. M. Heyes, Can. J. Phys. **64**, 773 (1986).
[26]D. M. Heyes and L. V. Woodcock, Molec. Phys. **59**, 1369 (1986).
[27]J. H. Dymond, Chem. Phys. **17**, 101 (1976).
[28]P. S. van der Gulik and N. J. Trappeniers, Physica B+C **139+140B**, 137 (1986).
[29]C. S. Murthy and K. Singer, J. Phys. Chem. **91**, 21 (1987).
[30]C. S. Murthy and K. Singer, Proc. R. Soc. A **389**, 299 (1983).
[31]N. J. Trappeniers, P. S. van der Gulik, and H. van der Hooff, Chem. Phys. Lett. **70**, 438 (1980).
[32]M. Bishop and J. P. J. Michels, Chem. Phys. Lett. **94**, 209 (1983).
[33]J. Kushick and B. J. Berne, J. Chem. Phys. **59**, 3732 (1973).
[34]J. P. J. Michels and N. J. Trappeniers, Physica **101A**, 156 (1980).
[35]M. Bishop, M. Derosa, and J. Lalli, J. Stat. Phys. **25**, 229 (1981).
[36]J. P. J. Michels and N. J. Trappeniers, Physica A **133**, 281 (1985).
[37]J. P. J. Michels and N. J. Trappeniers, Physica A **90**, 179 (1978).
[38]J. P. J. Michels and N. J. Trappeniers, Physica A **107**, 158 (1981).
[39]J. P. J. Michels and N. J. Trappeniers, Physica A **107**, 299 (1981).
[40]J. P. J. Michels and N. J. Trappeniers, Physica A **116**, 516 (1982).
[41]D. J. Evans, Phys. Rev. A **34**, 1449 (1986).